Influence of capping material upon biodegradation of polycyclic aromatic hydrocarbons in sediment-cap systems

by

Giovanna Pagnozzi M.S.

A Thesis

In

Civil Engineering

Submitted to the Graduate Faculty
of Texas Tech University in
Partial Fulfillment of
the Requirements for
the Degree of

MASTERS OF SCIENCE

Approved

Dr. Kayleigh Millerick
Chair of Committee

Dr. Danny Reible

Dr. Andrew Jackson

Mark Sheridan
Dean of the Graduate School

May, 2018

ACKNOWLEDGMENTS

This research project was partially funded by the Electric Power Research Institute, and I also want to acknowledge the department of Civil, Environmental, and Construction Engineering at Texas Tech University for the additional support.

I would like to express my deep gratitude to my adviser, Dr. Kayleigh Millerick, for her academic mentorship, and for always listening to my ideas and encouraging my research interests. I am highly grateful to my co-adviser, Dr. Danny Reible, for his guidance and expertise; he has been a constant source of valuable and helpful support. I am also thankful to Dr. Andrew Jackson for his constructive criticisms and advices.

My appreciation goes as well to the many persons that along this path offered help and support: Dr. Rakowska and Dr. Rao together with my colleagues Dimitri and Tariq for their expertise in analytical techniques, my labmates Asef, Andrew and Anastasia and all my fellow PhD students that shared with me classes and lab works.

Finally, I wish to thank my beloved family and my friends for their constant support and encouragement, throughout the years and the miles between us.

TABLE OF CONTENTS

ABSTRACT

Conventional capping strategies rely upon the physiochemical properties of capping media to sequester hydrophobic contaminants within sediments. This approach, a containment remedy, does not reduce overall contaminant mass. This study evaluates the potential for typical cap materials to provide a medium suitable for biodegradation, so that contaminants may be both sequestered and transformed. Bench top laboratory studies investigated biological activity in model systems consisting of conventional capping materials (granular activated carbon [GAC], organoclay, and sand), mineral media, pore water extracted from contaminated sediments, electron acceptors (oxygen, nitrate, sulfate and iron) and the electron donor, naphthalene (a model polycyclic aromatic hydrocarbon). Concentrations of and *nahAc* (a dioxygenase gene associated with aerobic transformation of naphthalene) in microcosms were monitored for 100 days. Experimental data were modeled and the relative kinetic rates were used to evaluate efficiencies of the different capping materials. Results show that GAC was the most successful of the capping materials investigated and facilitated naphthalene degradation in aerobic microcosms. The *nahAc* gene was sustained under these conditions. Some transformation of naphthalene was observed in aerobic microcosms prepared with sand and organoclay; however, kinetics were slow (sand) or not sustained (organoclay), and *nahAc* decreased in these systems. Less transformation was observed under anoxic conditions, but concentrations of naphthalene in GAC/nitrate microcosms were consistently below concentrations measured in sterilized controls, sand, and organoclay microcosms. To our knowledge, this work is the first to suggest that biodegradation of PAHs within sediment caps is significantly influenced by capping media selection.

LIST OF TABLES

LIST OF FIGURES

CHAPTER I

INTRODUCTION

Remediation of contaminated sediments has become in the past two decades an environmental issue of public concern. The risk associated with sediment contamination does not directly impact human health; therefore, contamination of sediments can be considered a chronic issue not likely to raise immediate awareness of the population. As a result, the legacy of contaminated sediments represents a challenge for remediation. The extent and volume of soil and water affected by contamination in sediment environments are considerably large, thus difficult to manage. In addition, several types of contaminants are characterized by a high affinity for organic carbon, resulting in a strong association with the natural organic fractions of fine-grained soil particles in sediments. The mobility of these fine-grained particles is usually very low; they accumulate in a stable zone of the sediment bed and facilitate slow, continuous diffusion of the contaminants in the overlaying water body. This results in persistent and resilient contamination, the grade and extent of which is defined by the nature of the pollutants.

Polycyclic aromatic hydrocarbons (PAHs) are ubiquitous contaminants of natural and anthropogenic origin, often associated with the contamination of sediments. PAHs are generated through three major processes that separate the compounds into three main classes: pyrogenic, petrogenic and biological (Abdel-Shafy and Mansour, 2016). Pyrogenic PAHs are formed either naturally from the combustion of organic matter at high temperatures under low to no oxygen conditions or by anthropogenic sources from the incomplete combustion of fuels. Petrogenic PAHs are generated from the maturation of crude oil, where their sources are either natural deposits or spills and wastes associated with human activities. Biological PAHs are usually released naturally by bacterial and algal synthesis during the degradation of vegetative matter. The chemical structure of PAHs consists of two or more fused benzene rings, characterizing molecules with a low solubility in water and a high affinity for organic carbon. These physicochemical properties of PAHs highly promote adsorption onto organic fractions

of sediments rather than the partition into the water column above. Therefore, sediments can act as sinks for those contaminants, slow diffusive zone forms that leads to the continuous release into aqueous or air phases at low but toxic concentration. Within the PAH family, 16 compounds have been identified by the EPA as priority pollutants based on their toxicity, dispersion in the environment and risk of exposure. Accumulation of those compounds in the environment can endanger both human health and the wellness of ecosystems because of their high toxicity, carcinogenicity and persistency (US EPA, 1984).

Remediation strategies for sediments contaminated by PAHs specifically aim at reducing the mass flux of contaminants to the water body and separating the benthic community (the ensemble of organisms living within the sediment bed) from the contamination source. The interaction between the contaminated sediments and the native benthic community causes the resuspension of the pollutants through bioturbation. In addition to increased mobility of the contaminants, the bioaccumulation will ultimately lead to trophic transfer. Bioturbation and bioaccumulation raise the risk associated with the contamination. The techniques used for remediation of sediment include dredging, capping and natural attenuation (Reible, 2014):

- Dredging, which consists of excavating and removing the first layer of sediments. The depth of dredging depends on the nature and extent of the contamination. Thus, the mass of contaminant is for the most part removed. However, this procedure perturbs the surface of the sediment bed and causes an initial resuspension of the contaminant, resulting in an increased mass flow to the overlaying water. In addition, the mixing at the sediment water interface alters the native benthic community and also any biodegradation activity, if it is present. Therefore, dredging initially magnifies the risk, but it reduces it in the long term because the contaminated portion of the sediments is removed. Consequently, dredging produces an amount of waste equal to the mass of sediments removed, which generates a secondary environmental issue related to disposal.

- Traditional sediment capping is an established practice to reduce the mass flux and delay the breakthrough of contaminants into overlying water bodies. Capping consists of the placement of one or more layers of an inert material on top of the sediment bed to create a barrier that retards the dissolution of the pollutants. Especially when contaminants show high affinity for soil particles, a well-designed capping system isolates the pollutants, efficiently shielding the sediments from erosion or resuspension and preserving the benthic community from interaction with the pollutants. Although capping attenuates the risk associated with sediment contamination in a relatively short time, it does not reduce the overall contaminant mass. Pollutants usually remain associated with the sediments, and leaks or aging eventually affect the overall efficiency of conventional capping.
- Natural attenuation is based on the principle of natural selection: an environment rich in contaminants can lead to the development of a microbial community able to metabolize pollutants as a carbon or energy source. Managing risk assessment of natural attenuation requires carefully evaluating the biodegradation capacity of the native microbial community. The decrease of the mass flux of contaminants to the overlaying water body depends mostly upon the kinetics of biodegradation related to the growth conditions within the sediments (mixing, reduction potential of electron acceptors and content of organic matter). An unfavorable environment hinders biodegradation rates, therefore limiting the application of natural attenuation as a remediation technique. However, natural attenuation has the potential to remove the contaminants without generating further environmental issues.

Currently, capping is considered a convenient and efficient practice to delay the dispersion of the pollutants into the environment and minimize the risk, although conventional capping does not remove the contamination. A capping system that promotes sequestration or degradation of the contaminants represents the optimal combination of risk containment and pollution removal. In the past decade, several studies focused on the development of a capping system that can actively or passively promote removal of contaminants, referred to as reactive capping.

The design of a reactive capping system substantially differs from conventional capping because a reactive capping system utilizes materials that interact physically or chemically with the contaminants. A physical process like adsorption contributes to the removal of contaminants from environmental compartments (sediments and water) via segregation onto adsorbent materials. The addition of one or more layers of capping materials with adsorbent capacity transforms a conventional cap into a reactive cap that sequestrates the contaminants and prevents their dispersion in the environment. The utilization of adsorption as separation technique is particularly efficient for organic compounds like PAHs. The high affinity for organic carbon promotes adsorption of those contaminants on different materials like organoclay and activated carbon (Reible et al. 2006, Smith et al. 2006, Park et al.2011, Sarkar et al. 2012, Gilmour et al. 2013; Millward et al. 2005; Murphy et al. 2006; Werner et al. 2005). The characteristics of the contaminants play a major role in the capability of designing reactive capping, since the physicochemical properties determine which separation processes are effective in removing the compounds. Capping materials with ion exchange capacity have been employed to sequester heavy metals, as metal species exist in different charged forms when dissolved in aqueous solutions. Zeolites and phosphate minerals have been incorporated into reactive capping systems to stabilize and remove metals (Baker et al.2009; Erdem et al. 2004; Hamidpour et al. 2010; Mahabadi et al. 2007; Wingenfelder et al. 2005).

Immobilization of contaminants onto reactive capping media removes the bulk of the contamination from a risk-sensitive environmental matrix (sediment and water), but contains the contamination in a new medium (the capping material). Contaminant release from the capping matrix, caused by leaks, aging, or desorption processes, can impact the efficiency of the containment system. The ideal solution is to design a reactive capping system with materials able to promote degradation processes that convert the contaminants into benign products. The use of a well-developed reactive material like zero valent iron is currently the best example of a successful chemically reactive capping system (Kanel et al. 2005; Kržišnik et al. 2014; Petersen et al. 2012).

However, the development of reactive capping materials presents technical and logistical difficulties to overcome. If capping can also provide a suitable medium for propagation of a native microbial community capable of degrading the contaminants, design challenges of containment can be relaxed, as biological processes have the potential to reduce (or even eliminate) long-term pollutant releases from capping systems.

The native microbial community of a contaminated site can contain a certain percentage of microorganisms able to biotransform or even biologically mineralize the contaminants. The rate and extent of biotransformation and biodegradation are highly variable and depend upon the characteristics of the sediments and the properties of the contaminants. The occurrence of biodegradation within sediment capping environments has been observed, usually with sand as capping media. Biodegradation of chlorinated solvents was demonstrated in sediments and porewater within packed sand columns designed to simulate caps (Himmelheber et al. 2011). Hyun *et al.* demonstrated at laboratory scale that bio-reactive zones can form in sand, resulting in the biodegradation of PAHs in coal tar-contaminated river sediment. Some biodegradation was also observed in situ using test cell cylinders that monitored concentration gradients and fluxes through sand and organoclay caps in river sediments contaminated with coal tar (Kim et al. 2014). An electrode-enhanced sand cap has been proven to stimulate PAH biotransformation by increasing the redox potential (Yan et al., 2015). An effective bio-reactive capping system will aim to contain contaminants while promoting and sustaining the growth of the native microbial community able to degrade the pollutants. Schematic differences between conventional, reactive and bio-reactive capping systems are illustrated in Figure 1.

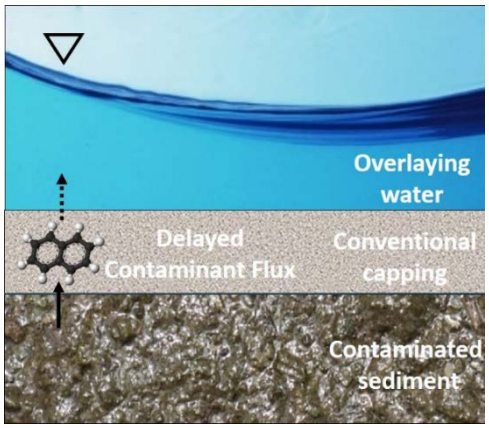

Conventional capping confines the contamination to the sediments and prevents erosion and resuspension; it delays the mass flux of contaminant to the overlaying water.

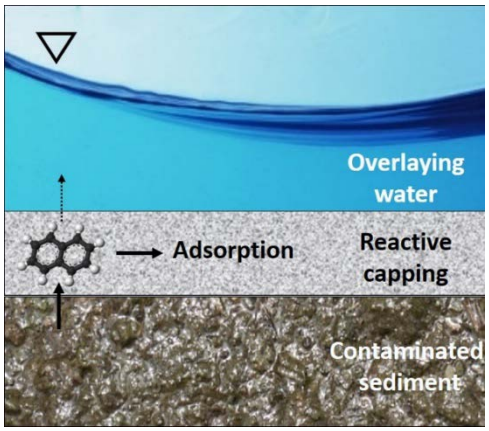

Reactive capping consists of one or more layers of adsorbent or reactive materials that sequestrate the contaminants; it decreases and delays the mass flux of contaminant to the overlaying water.

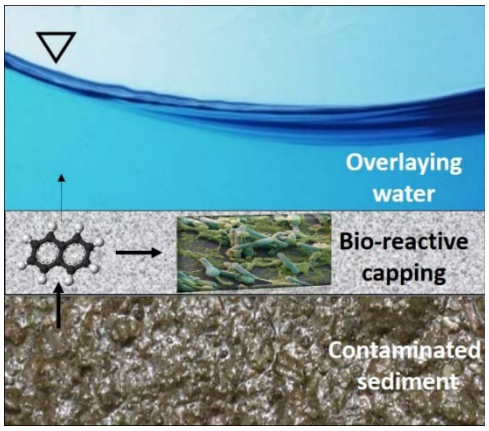

Bio-reactive capping consists of materials that sustain and promote the growth of native microbial communities able to degrade the contaminants; the mass flux to the overlaying water is delayed, and the pollutants are degraded within the capping system.

Figure 1: Schematic representation of capping systems.

The challenges in designing a bio-reactive capping system lie in the necessity to enhance a reaction that, in non-ideal conditions, can exhibit non-observable kinetics. The optimal environment for a specific consortium of microorganisms requires that several parameters, such as concentration of available substrate, redox potential, pH and temperature, must remain in a certain range. Those conditions may largely fluctuate in a contaminated site and the likelihood for the biodegradation mostly depends on a combination of variables. The capability of a capping material to serve as suitable media for the growth of a community of biodegraders could greatly influence the feasibility of a bio-reactive capping system. Whether the presence of a capping system on top of the sediment bed can or cannot stimulate the biological processes present in situ has not been investigated.

Biodegradation of PAHs has been reported in previous studies (Fogh, 2008; Carmona et al., 2009 and Seo et al., 2009). Due to its small size and affinity for the aqueous phase, naphthalene ($C_{10}H_8$) is the most likely of the PAHs to migrate within active capping systems. It is also the most readily biotransformed, making it an ideal target compound for bio-reactvive capping. Biodegradation of naphthalene in non-capping environments has been reported in both anaerobic (Rockne et al. 2001, Kummel et al. 2016, and Anderson et al. 2009) and aerobic conditions (Peng et al., 2008).

Naphthalene biodegradation in anaerobic conditions is not well understood and the genes encoding for the enzymes involved have not been clearly identified. The proposed pathway starts with the activation of naphthalene through formation of a succinate coenzyme A intermediate that is further reduced (Meckenstock et al. 2016). However, further studies are necessary to determine the sequence of reactions and the genes involved. The biodegradation of naphthalene in aerobic conditions follows a well-defined pathway. Naphthalene degradation is initiated through the addition of two hydroxylic groups by a dioxygenase enzyme. The formed intermediate is broken down to salicylate and enters the tricarboxylic acid cycle. The genes involved have been well characterized for the catabolic pathway encoded by the plasmid NAH7 in *Pseudomonas*

putida G7 (Sota et al., 2006). The NAH7 plasmid contains two operons codifying for the structural genes of the aerobic naphthalene degradation pathway. The first one contains the gene for the enzymes responsible for the transformation of naphthalene to salicylate, the second one encodes enzymes involved in the salicylate reduction process. Within the first operon, the *nahAc* gene codifies for the naphthalene dioxygenase, and it has been used as biomarker to study PAH biodegradation activity (Park et al. 2006, Nyyssonen et al. 2008, Baldwin et al. 2008, Cebron et al. 2008).

This research aims to experimentally evaluate the extent to which capping media selection affects bioactivity in model capping systems. Specifically, this work:

1) Monitored naphthalene biodegradation and compared reaction kinetics in the presence of different capping materials.
2) Examined the extent of naphthalene decay due to biological processes under different electron accepting conditions.
3) Determined naphthalene biodegradation activity in laboratory microcosms through the quantification of the *nahAc* gene.

Experiments mimicked sediment cap environments using laboratory microcosms. Naphthalene concentrations and the *nahAc* gene (biomarker) were monitored over time. This study evaluated a matrix of variables, including three different capping materials and four different electron-accepting conditions. Finally, the rate constants for the biodegradation processes were estimated. Biotransformation kinetics and abundances of catabolic gene were compared to provide practical recommendations for designing bio-reactive caps.

CHAPTER II

MATERIALS AND METHODS

Sediments

PAH-contaminated sediments were obtained from a contaminated site in the Midwestern United States. At the time of sampling, sediments were screened visually (no NAPL observed) and with a PID (readings between 5 and 18 ppm). The sediments were shipped to Texas Tech University on August 4th, 2015 and were stored at 4 °C. The sediments remained sealed until immediately before use. Once opened, the sediments appeared gray in color, silty, and had a moderate odor of petroleum hydrocarbons. Sediment was evaluated for total organic carbon (TOC), moisture content, polycyclic aromatic hydrocarbons (PAH), total DNA, and naphthalene-degrading bacterial genes. Sediment-specific methods are described below.

Quantification of total organic carbon (TOC) and moisture content.

Sediment samples were dried in the oven at 105 °C overnight, stored in a desiccator to cool down, and homogenized. The samples were weighed, and moisture content was determined by difference between values obtained pre and post oven treatment. A quantity of 5-10 mg of sediment was placed in silver boats and inorganic carbon was removed with hydrochloric acid (37%) for an incubation time of 4 hours at room temperature. Treated samples were dried (1 h at 105 °C), placed in tin boats, palletized and analyzed for TOC using a Vario TOC Select (Elementar).

Determination of PAH content.

Sediments were dried at 35 °C for 24 h, until a moisture content of ~20% was reached. Polycyclic aromatic hydrocarbons were extracted from sediments using Accelerated Solvent Extraction (ASE 350, Dionex, USA) with a mixture of dichloromethane/hexane (4:1, v/v) at 100°C. Two extraction cycles of 5 min each were used in the procedure. Sediment samples were cleaned up with silica and copper in an

extraction cell. Additional external cleanup was performed by eluting the samples with hexane through a column packed with sodium sulfate and aluminum oxide (Al_2O_3). Extracts were further concentrated to 1-1.5 mL, exchanged to acetonitrile and analyzed for PAHs using high performance liquid chromatography (HPLC, see Analytical methods section).

DNA extraction from sediment.

Soil DNA (0.25 g wet soil) was extracted using a PowerSoil DNA isolation kit (MoBio Laboratories, Carlsbad, CA), in accordance with the manufacturer's instructions. Following extraction, total DNA was quantified using Qubit™ and analyzed for presence of the naphthalene-degrading bacterial gene *nahAc* using qPCR. These methods are described further in Analytical methods section.

Porewater

Porewater was extracted from river sediments through centrifugation at 5000 rpm for 20 minutes at room temperature.

Quantification of dissolved organic carbon (DOC).

Porewater was filtered through a 0.2 µm PTFE filter prior to analysis to prevent instrument clogging. To remove inorganic carbon, samples were titrated with hydrochloric acid (37%) until acidified ($pH \leq 2$). This converted all inorganic carbon into carbonic acid, which was removed via purging. After acidification, triplicate porewater samples (20 mL) were analyzed using a Vario TOC Select (Elementar). DDI blanks, standards (2-20 mg/L, prepared with potassium hydrogen phthalate [KHP] and DDI), and a quality control sample were analyzed to evaluate the integrity of the method.

Determination of PAH content.

After filtration through a 0.2 µm PTFE filter (to prevent instrument clogging) pore water samples were directly diluted with 97% acetonitrile. Samples were analyzed

for PAHs using high performance liquid chromatography (HPLC, see Analytical methods section).

DNA extraction from porewater.

Aqueous DNA extractions were performed using 10 mL of porewater and a QuiAmp DNA mini kit (QIAGEN Technologies) in accordance with the manufacturer's instructions. Following extraction, total DNA was quantified (Qubit™) and analyzed for the presence of the naphthalene-degrading bacterial gene *nahAc* (qPCR).

Enriched cultures

Microbial communities were enriched from the contaminated sediments prior to microcosm setup. This approach was used to increase the number of bacteria in the liquid phase, to adjust bacteria to the selected electron accepting conditions, and to avoid direct inoculation using river sediments, which would have complicated comparisons between capping materials. Six cultures were enriched; five contained naphthalene and electron acceptor (oxygen, nitrate, sulfate, iron, or no acceptor). The sixth contained no naphthalene or electron acceptor (control). Electron acceptors were supplied in excess of the total mass of naphthalene added, per the following reactions:

Oxygen: $C_{10}H_8 + 12O_2 \rightarrow 4H_2O + 10CO_2$ **(1)**

Nitrate: $\frac{1}{48}C_{10}H_8 + \frac{1}{5}NO_3^- + \frac{1}{5}H^+ \rightarrow \frac{11}{60}H_2O + \frac{1}{10}N_2 + \frac{10}{48}CO_2$ **(2)**

Sulfate: $\frac{1}{48}C_{10}H_8 + \frac{1}{8}SO_4^{2-} + \frac{1}{4}H^+ \rightarrow \frac{1}{12}H_2O + \frac{1}{8}H_2S + \frac{10}{48}CO_2$ **(3)**

Iron: $\frac{1}{48}C_{10}H_8 + FeOOH + 2H^+ \rightarrow \frac{19}{12}H_2O + Fe^{2+} + \frac{10}{48}CO_2$ **(4)**

Final electron acceptor concentrations were 10 mM ($NaNO_3$), 20 mM (FeOOH, prepared as previously described (Kwon et al., 2008), and 20 mM (Na_2SO_4). Oxic microcosms contained 0.123 mmoles O_2. Each electron acceptor was present in excess of the stoichiometric requirement necessary to oxidize naphthalene to CO_2. Enrichment

cultures contained sediment (25 g), porewater (10%), and 30 mM HCO_3 buffered media (52 mL) (Vogt et al., 2007). Electron acceptors were amended from concentrated stock solutions in degassed, deionized water or not degassed (oxic). Once prepared, enrichments were purged to remove O_2 (80:20 N_2/CO_2; all enrichments except O_2), amended with naphthalene (1 mg/L) and sealed. Cultures were incubated for 58 days at room temperature and kept continuously agitated (100 rpm). Two controls were also prepared: control 1 contained electron donors, naphthalene, but no acceptor; control 2 contained neither naphthalene nor acceptor.

DNA extraction from enriched culture.

The sediment slurry (0.5 g) was condensed via centrifugation at 10,000 rpm for 10 minutes at room temperature. The supernatant was decanted, and the pellet was resuspended using the solution from the power bed tubes of the PowerSoil DNA isolation kit (MoBio Laboratories, Carlsbad, CA). Following this steps DNA extraction was performed in accordance with the manufacturer's instructions (starting from step 3 of the protocol). Samples were then evaluated for total DNA (Qubit™), and presence of naphthalene-degrading bacterial genes (qPCR). All biological samples were archived frozen (– 20°C) for possible additional testing.

Microcosms

Capping microcosms were setup in triplicate using 30 mL borosilicate glass vials sealed with thick butyl stoppers lined with Teflon. Microcosms contained capping material, media, porewater, buffer, electron acceptor, and naphthalene. The detailed composition of each microcosm triplicate is reported in the Appendix (Table A.1-A.3).

Capping materials.

Microcosms included three different capping materials: granular activated carbon (BPL® 4x10, Calgon Carbon), organophilic clay (Organoclay® PM-199 CETCO) and fine white sand (S25516, Fisher Scientific). Capping material masses were determined using isotherms generated during previous studies and designed. Given the

isotherm calculations and mass phase distributions (further discussed in this section), capping masses used were 5 mg (GAC) and 668 mg (sand and organoclay). Materials were washed twice with DI water and dried overnight at 35°C before they were added to microcosms.

Media and pore water.

Mineral media containing salts, vitamins, and trace elements was prepared as described by Vogt et al. and sterilized by autoclaving (120 °C, 20 minutes). Media was blended with porewater (12% porewater [v/v]), dispensed into microcosm vials containing capping materials, and purged with anoxic gas (N_2). A bicarbonate buffer (1 M stock) was prepared separately, purged with anoxic gas (N_2/CO_2 [80:20]) and sterilized through autoclave. The buffer was added anoxically to microcosms via syringe to maintain neutral pH (amended to a final concentration of 30 mM and final pH ~7.2).

Electron acceptors.

Electron acceptors were added to degassed, buffered microcosms via headspace (oxygen) or as amendments from concentrated stock solutions in deionized water (iron, sulfate, or nitrate as electron acceptor). Concentrated stock solutions were degassed with nitrogen and sterilized prior to amendment. “No acceptor” controls were prepared identically except were not amended with any acceptor. Microcosms intended as sterile controls were autoclaved prior to naphthalene amendment. Experimental microcosms were prepared with sterilized media and electron acceptors, but they were not autoclaved after assembling.

Naphthalene partitioning.

Naphthalene was amended into microcosms from a concentrated solution. Stock solution was prepared by dissolving solid-phase naphthalene into 100% acetonitrile at final concentration of 40 g/L (confirmed by HPLC analysis prior to amendment); the purpose of a highly concentrated stock was to minimize the volume of toxic acetonitrile

in microcosms. Naphthalene amendment was performed prior to inoculation and Day 0 sampling of the microcosms. Partitioning and distribution of naphthalene in each system was estimated using equation **(5)**:

$$Mass_{naphthalene} = C_w H V_a + C_w V_w + K_{oc}\rho_{doc}V_{doc} + q_e Mass_{capping} \quad \textbf{(5)}$$

H represents the Henry's constant for naphthalene (0.0223 C_a/C_w; estimated using ARChem's physicochemical calculator SPARC); C_w is the aqueous concentration of naphthalene; V_a is the volume of headspace (5 mL); V_w is volume of the aqueous phase (25 mL); V_{doc} is the volume of dissolved organic carbon (3 mL); K_{OC} is the organic carbon partitioning coefficient ($10^{3.04}$ L/Kg, (Montgomery, 1990)); ρ_{OC} is the density of the dissolved organic carbon (2.6 g/cm^3). Given the different adsorptive properties of capping materials used, the following equations were used to estimate masses of naphthalene adsorbed:

- the Freundlich isotherm below (Dunlap, 2011)was used for activated carbon:

$$q_e = 34.37 C_w^{0.21} \textbf{ (6)}$$

- the organic carbon/water partitioning coefficient of naphthalene and the organic content of the capping material describe the adsorption onto sand and organoclay:

$$q_e = K_{OC} f_{OC} C_w \textbf{ (7)}$$

In these equations, q_e is the mass of naphthalene adsorbed onto the capping material [units are mg naphthalene/g **(6)** and mg naphthalene/L **(7)**]; C_w and K_{oc} are the same as **(5)**, and f_{OC} is the fraction of organic carbon (1 for organoclay, 0.01 for sand).

The mass of naphthalene added to each system was 0.758 mg, supporting calculations are reported in Appendix (Table A.4). While the mass of naphthalene was kept fixed, the mass of capping material was back-calculated to achieve aqueous naphthalene concentrations of 1 mg/L (GAC and organoclay) and 3 mg/L (sand). At equilibrium, the aqueous phase represents 3.3% of the total naphthalene in GAC and organoclay and 10.2% in sand microcosms (most naphthalene will be adsorbed).

Inoculum and sampling schedule.

Microcosms were equilibrated for 7 days (GAC) or 24 hours (all others) after the amendment with naphthalene. Following equilibration, 1.25 mL aliquots of the enrichment cultures were used to inoculate prepared microcosms via syringe. Microcosms were sampled for polycyclic aromatic hydrocarbon concentrations and/or *nahAc* genes at 0, 14 (oxic microcosms only), 35, 56, 70, and 100 days (sampling point at Day 100 for anoxic microcosms only).

PAH quantification in microcosms.

Aqueous samples (1 mL) were extracted using a syringe previously purged with N_2 to maintain anoxic conditions. The samples were filtered through a 0.2 µm PTFE syringe filter and preserved in acetonitrile (ratio of 97:3 [acetonitrile:sample]) prior to analysis using high performance liquid chromatography.

DNA extraction in microcosms.

Neither conventional soil extraction (microcosms were predominantly liquid) nor liquid extraction (microcosms contained capping materials that could be colonized) were appropriate for our microcosms. To extract DNA, samples were sacrificed, condensed using centrifugation and amended as a thick slurry to soil bead beating tubes. Following extraction, samples were evaluated for total DNA (Qubit™), and presence of aerobic naphthalene-degrading bacterial genes (qPCR). All biological samples were archived frozen (– 20 or – 80°C) for possible additional testing.

Analytical methods

Determination of PAH concentrations.

Samples were analyzed using high performance liquid chromatography (HPLC, Agilent 1200) equipped with a UV-Diode array detector and a fluorescence detector and using a modified version of EPA method 8310. The method utilized an isocratic mobile phase of acetonitrile:ultra-pure water [70:30] and a Phenomenex Luna® 5 µm C18 column (250 x 4.6 mm). Naphthalene eluted at approximately 8 minutes, was measured

via fluorescence. This method can also quantify thirteen other polycyclic aromatic hydrocarbons, and initial sediment and porewater samples were screened for these other compounds in addition to naphthalene. Naphthalene standards ranging from 0.5 to 200 µg/L in acetonitrile were prepared from a 1000 mg/L PAH16 stock solution (Ultra Scientific, Kingstown, RI). A nine point calibration led to a linear calibration with $R^2 >$ 0.999 for all compounds.

DNA quantification.

Total DNA (10 µL of DNA extract) was quantified using a Qubit™ 3.0 fluorometer (Life Technologies) and the Qubit™ high sensitivity DS DNA assay. DNA standards (0-10 ng/µL) were used to derive a calibration curve for sample quantification.

Quantification of the *nahAc* gene.

Quantification of *nahAc* gene was conducted as described in a previous study (Cèbron et al. 2008). Real-Time PCR was performed in 20 µL reaction volumes containing SYBR Green Supermix (Bio-Rad), 0.1 µM of each primer, and 6 µL of template DNA (standards, environmental samples, or DNA extracted from *Geobacter sulfurreducens* strain PCA [negative control for the *nahAc* gene]) or distilled water (blank). Primers are specific to PAH-degrading genes on gram negative bacteria and standards were purchased from Integrated DNA Technologies, IDT, as an oligonucleotide synthesis product; detailed information reported in the Appendix. Resulting amplicons correspond with the *nahAc* gene on *Pseudomonas putida*, and our results are reported as copies of *nahAc*. The gene fragment was shipped in lyophilized form, resuspended in TAE buffer and activated following manufactory instructions. DNA concentration was determined by nanodrop spectrophotometer analysis prior to amplification. Standards were serially diluted in TAE buffer, and a nine-point calibration led to a linear calibration (Figure A.1 in the Appendix). No amplification or fluorescence was observed in blanks or negative DNA controls, confirming primer specificity to PAH degrading bacteria. The amplifications were carried out with the following cycling sequence:

Initial heating to 95 °C, for 5 min

The following sequence repeated for 50 cycles: {(30s at 95°C@30s at 56°C @30s at 72°C@10s at 80°C)}

A final holding step at 72 °C, for 7 min.

Following amplification, a melting curve analysis was performed by measuring SYBR Green signal intensities during a 0.5 °C temperature increment every 10 s from 51 °C to 95 °C. Following qPCR, results were exported for further analysis.

CHAPTER III

RESULTS

Characterization of sediments and porewater samples

Sediments were characterized prior to use. Total organic carbon content was 2.75% and the moisture content was 47% (± 1.5%). Dissolved organic carbon in porewater was 91.29 ± 5.24 mg/L. Naphthalene was the most abundant hydrocarbon recovered from sediments (10,475 µg/kg, 31.6% of total PAHs), and all PAHs (including naphthalene) were below detection limits in porewater (Table A.5 in the Appendix). The total concentration of *nahAc* recovered (from 0.25 g sediments, concentrated to 100 µL of extract) with the PowerSoil DNA isolation kit was 1.38×10^6 copies/µL (standard deviation of $\pm 2.0 \times 10^4$).

Baseline of naphthalene concentrations

Baseline sampling occurred after an equilibration period and before the inoculation with the enrichments. The equilibration period was necessary to overcome dissimilarities in adsorption kinetics due to the different characteristics of the three capping materials. Equilibration times (7 days for GAC and 24 hours for organoclay and sand) were estimated using data from previous experiments with PAHs and these media types. The target concentrations were set to estimate the mass of naphthalene that, once at equilibrium, partitioned in the different compartments of the system (capping, organic matter, air and water), thus resulting in the desired concentration in the water phase. The baseline in autoclaved controls, shown in Figure 2, closely resembled target concentrations of 1 mg/L (GAC and organoclay) and 3 mg/L (sand). This showed that i) equilibrium equations (Equations 5-7) and ii) equilibration time estimates were both valid for this system. In the figure, the target concentrations are represented with a dashed horizontal line.

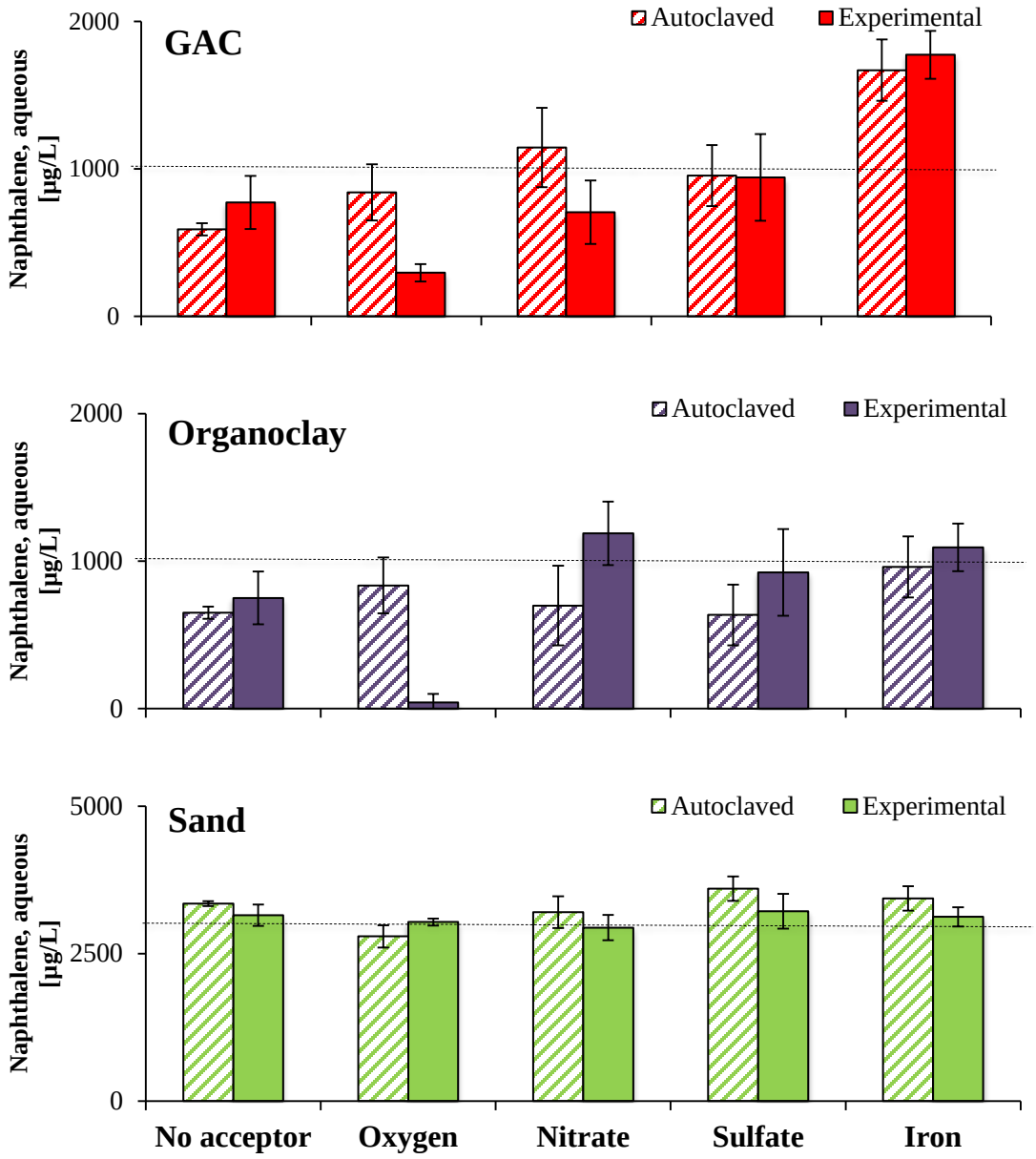

Figure 2: Baseline naphthalene concentrations. GAC (red), organoclay (purple), and sand (green) microcosms. Solid bars represent experimental, while striped bars correspond to autoclaved microcosms. Dashed lines indicate the targeted naphthalene concentration.

Baseline values in GAC/iron hydroxide sterile microcosms were 50% higher than expected. The iron solution used is a thick, highly viscous substance colloquially

referred to as “iron gel”. Although the iron disperses in water when amended into aqueous solutions, the dense mixture may have interacted with GAC pores and caused pore blockage.

The initial naphthalene concentrations in several GAC non-sterile microcosms were lower than expected. Baseline data were taken after the equilibration period, but before inoculation with enriched culture. Losses of naphthalene due to biotransformation during the adsorption equilibration period can explain discrepancies between autoclaved and experimental GAC microcosms (oxic and nitrate). Decreases of naphthalene concentrations in experimental microcosms (compared against the autoclaved controls) suggest presence of biological activity in porewater. While all microcosms were amended with porewater, vials intended as sterile controls were autoclaved a second time after porewater addition, but experimental vials were not. This was: i) To keep porewater as consistent as possible with in situ conditions, and ii) Because porewater was not expected to be a significant source of bioactivity, as abundance of *nahAc* gene was two order of magnitude lower in porewater than in inoculation enrichment (5,106 copies/10 µL compared with 546,000 copies/10 µL for oxic enrichments).

Naphthalene degradation due to biological activity before the inoculum introduces an additional variable into these systems, since the equilibration time was different for GAC and organoclay-sand microcosms. However, the naphthalene time series exhibited a defined decay pattern in GAC systems over 70 days (well beyond this initial 6 days difference). Asymptotic naphthalene behavior was observed in later time points for microcosms containing other capping materials.

Losses of naphthalene during the equilibration period were reported in autoclaved microcosms containing organoclay. This can be explained by a partial deterioration of the adsorbents during autoclaving. One study showed that heavy thermal treatment can affect the sorptive properties of organoclay (Borisover M. et al., 2010). In our data, the time zero value of the oxic-organoclay experimental samples

showed naphthalene concentrations substantially lower than the sterile microcosms (<10% of the control). While peculiar, this data was not considered significant because it was inconsistent with further samplings (values at Day 14 are higher than baseline for those microcosms, and this trend continues throughout the experiment).

Assessment of naphthalene decay in sediment-capping microcosms

Naphthalene concentrations were monitored for 70 days in oxic microcosms and 100 days in anaerobic systems; these data are reported in detail in the Appendix (Table A.6-A.8). Figure 3 shows the naphthalene concentration time series for each electron acceptor. The measured naphthalene concentrations were normalized to the average of the relative sterile triplicates at each time point, and errors were estimated according to the propagation of errors formula, provided in the Appendix (equations 10-12). Time courses showing naphthalene concentrations in log scale are also reported to emphasize extent of naphthalene decay (right column).

Naphthalene decreased most rapidly under aerobic conditions; this was expected due to higher specific bacterial growth rates within the microcosms, as result of the catabolic reducing potential of oxygen (Eriksson et al., 2003). For this reason, oxygen microcosms were sampled during a shorter time, which meant that all three microcosms were sacrificed for final biological sampling on Day 70, not Day 100 as for anoxic microcosms. The most significant change in naphthalene over the 70 days (compared with controls) occurred in GAC microcosms, with errors consistently under 20%. Data show that naphthalene concentrations in oxic experimental microcosms are uniformly lower than the sterile controls for all three capping material types. Naphthalene in GAC/oxic microcosms steadily decreases from Day 14 forward, and naphthalene at Day 70 in the GAC/oxic microcosm is only 0.68% of the concentration in the corresponding sterile control.

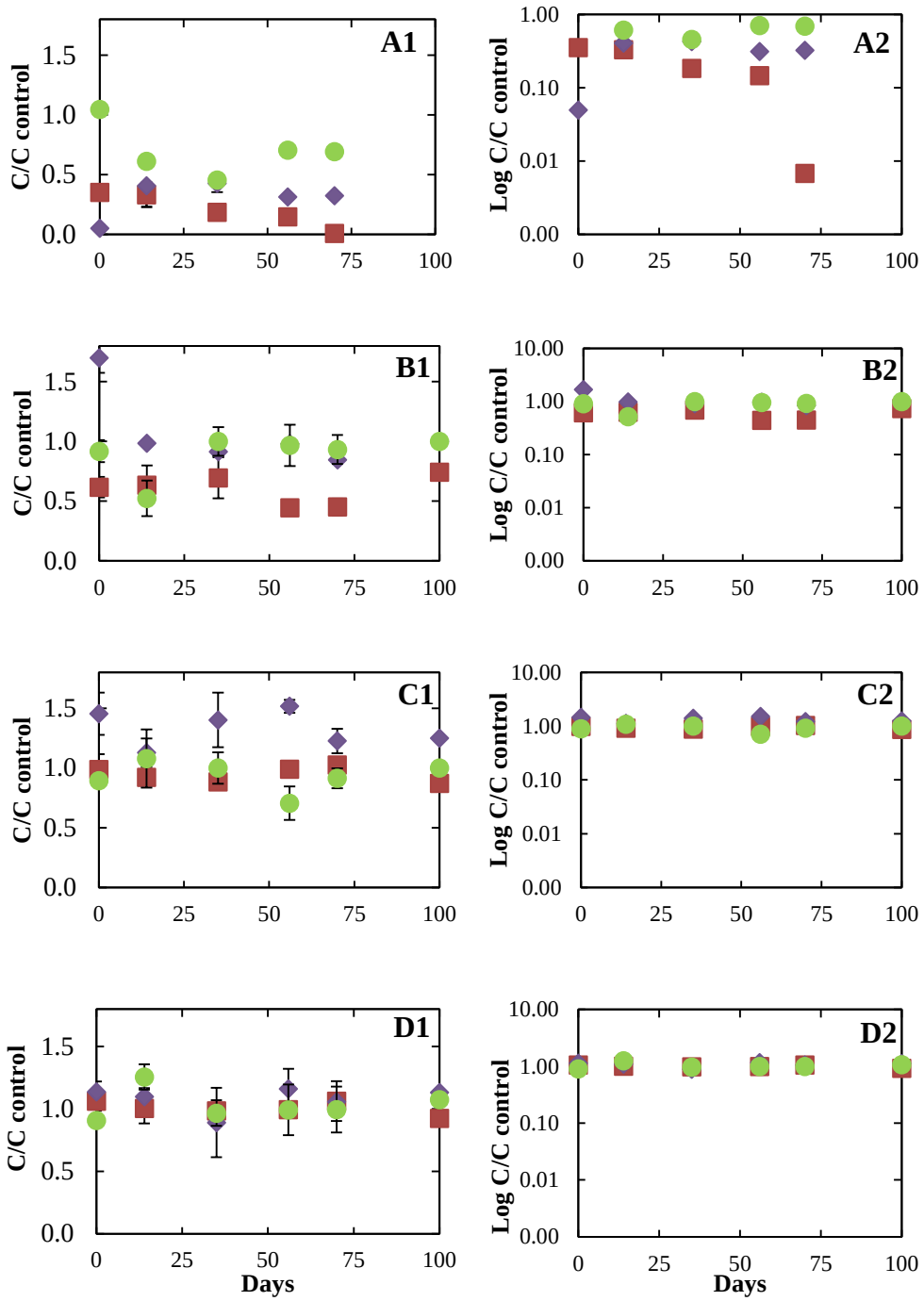

Figure 3: Time series of naphthalene concentration. **A** shows oxygen amended microcosms, **B** nitrate, **C** sulfate and **D** iron hydroxide. Logarithmic scale on the right. The graphs report data for microcosms prepared with GAC (■), organoclay (◆) and sand (●).

The decay trend of GAC microcosms is more clearly defined in the logarithmic plots. Patterns are less clear for oxic microcosms containing organoclay and sand. Naphthalene in organoclay microcosms is ~40% of controls at all time points, except for the initial drop at baseline sampling, and sand microcosms showed some naphthalene decay but with high variability. Overall, naphthalene ratios in sand and organoclay microcosms behave mostly asymptotically from Day 14 onwards.

Less transformation was observed under anaerobic conditions over the 100-days experiment. Concentrations of naphthalene in GAC/nitrate experimental microcosms fluctuated between 45% and 74% of the concentrations measured in sterilized controls. The trend in sand/nitrate systems is constant; ratio values are ~ 1.0, except for one time-point (52% at Day 14) that cannot be considered statistically significant because of the high variability between duplicate samples.

Naphthalene concentrations in sulfate and iron experimental microcosms were consistently very similar to the sterilized controls. Minimal naphthalene decay was expected for sulfate and iron-reducing microcosms, due to slow biodegradation kinetics. Furthermore, the environment in these microcosms could have become microaerophilic (instead of anaerobic), due to repeated sampling of the same serum bottle. This would have caused arrested growth of either sulfate reducing or iron reducing bacteria, which are strictly obligate anaerobes.

First-order biological decay constant and ANOVA analysis

Sediment-cap microcosms were sampled for naphthalene concentrations by puncturing the butyl stoppers that sealed the serum bottles with a syringe. Stoppers were coated in Teflon to minimize losses, but repeated sampling may have punctured the Teflon layer, exposing the butyl material that could serve as a naphthalene adsorbent. To test this hypothesis, control systems mimicking the microcosms but containing only water and naphthalene were monitored over time for naphthalene concentrations.

These experiments showed that naphthalene concentrations decreased throughout the observation time of 100 days (Table A.9 in the Appendix). Data collected were fitted to a linear regression model, according to the linearized 1st order decay expression:

$$lnC = lnC_0 + kt \quad \textbf{(8)}$$

Coefficients were estimated with analysis of variances, and statistics are reported in the Appendix (Table A.10). The equation obtained is:

$$lnC = -0.0098t + 7.6242 \quad \textbf{(9)}$$

Data collected for microcosms were modeled as described for the control test using **(8)**, except i) microcosms that did not have at least four HPLC analysis points were excluded, and ii) data series that produce R^2 fit values of 0.65 or lower were excluded. and $k_{observed}$ were estimated through ANOVA. Biological sampling required sacrificing microcosms, so not all microcosms had four data points. For all series except oxic series, this meant that two of the three triplicates could be used to calculate $k_{observed}$. For oxic microcosms (sampled at Day 14 for *nahAc*), only one triplicate in each series had the minimum number of data points.

Decay rates are presented in Table 1. Only one (n = 18) GAC series did not meet the R^2 value of 0.65 (the R^2 value in this system was 0.26); this was a sterile microcosm under nitrate-reducing conditions with erratic naphthalene concentrations. Three (n = 18) sand series did not meet R^2 values of 0.65; this included one sterile iron, one experimental iron, and one sterile sulfate microcosm. $k_{observed}$ for microcosms containing organoclay are not included because greater than 50% of organoclay microcosms did not follow first order decay and generated R^2 fit values of 0.50 or lower. All data points exceed the $k_{control}$, suggesting continued loss of naphthalene over 100 days to capping material or DOC. The rate constant $k_{control}$ was compared against the constants observed in microcosm studies.

Table 1: Observed first order decay constants [$k_{observed}$, day^{-1}]

	No Acceptor	***Oxygen***	***Nitrate***	***Iron***	***Sulfate***
Sterile GAC	0.0127	0.0145	0.0136	0.0125	0.0156
p-value	0.0005	0.0106	0.0077	0.0002	0.0003
GAC	0.0141	0.0604	0.0187	0.0131	0.0165
p-value	0.0006	0.0095	0.0035	0.00004	0.0002
Sterile Sand	0.0149	0.0170	0.0149	0.0110	0.0131
p-value	0.0016	0.0897	0.0042	0.0460	0.0444
Sand	0.0135	0.0193	0.0148	0.0123	0.0146
p-value	0.0015	0.1274	0.0019	0.0073	0.0024

The statistical significance of the data used to generate the first order decay constants presented in Table 1 was assessed using the analysis of variance (ANOVA) method and relative p values are listed. Of the $k_{observed}$ values presented, only the GAC/oxic microcosms were significantly different from other $k_{observed}$ values at a 95% confidence interval. While this does not exclude the possibility of slow degradation rates in the other microcosms, it does suggest significant biological transformation in GAC/oxic microcosms.

One limitation of this study is that only 3.3% of the total naphthalene was in the aqueous phase in the sediment cap systems containing GAC and organoclay, and 10.2% for sand, as shown in Table 2. Since a high percentage of the total naphthalene in the system was adsorbed (~97% for GAC and organoclay, ~90% for sand), gradual decreases in naphthalene concentrations in the aqueous phase may have been obscured by desorption of naphthalene from the adsorbed phase. This scenario could result in naphthalene concentrations that appeared asymptotic compared with controls, even if relatively slow degradation was occurring.

Table 2: Naphthalene mass distribution in environmental compartments.

	Cwater mg/L	Mwater mg	Mair mg	Mcapping mg	Morganic carbon mg	Total Mass mg	% of Total Mass in Water
GAC	1	0.025	0.0001	0.733	0.0003	0.758	3.298
Organoclay	1	0.025	0.0001	0.733	0.0003	0.758	3.298
SAND	3	0.075	0.0003	0.660	0.0003	0.735	10.204

Naphthalene catabolic gene quantification

Microcosms were analyzed for the *nahAc* gene during baseline sampling and at three other time points (since sampling required sacrificing a triplicate, only three data could be taken in this study). Total DNA concentrations in the extracts and gene abundances are reported in the Appendix (Table A.10-A.12). Under oxic conditions, *nahAc* copy numbers were consistently above initial values in microcosms containing GAC or sand, contrary to unspiked controls which did not exhibit differences from the baseline, as shown in Figure 4.

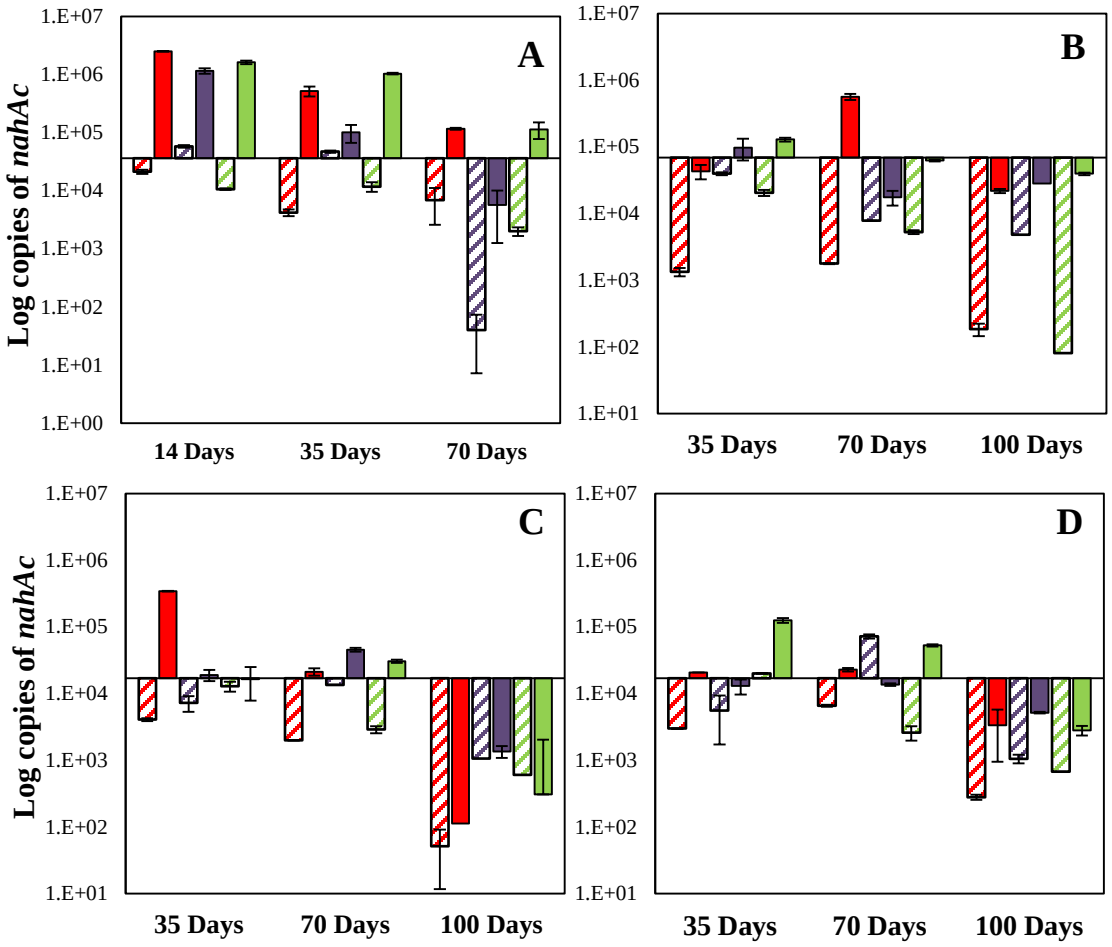

Figure 4: Changes in *nahAc* gene abundance. Copy numbers are reported per 10µL DNA extract. **A** shows oxygen amended microcosms, **B** nitrate, **C** sulfate and **D** iron hydroxide. Solid bars correspond to experimental microcosms and striped bars represent controls not amended with naphthalene. Red corresponds to GAC microcosms, purple for organoclay, and green for sand.

The increase in gene copy numbers suggests that sand and GAC may be a suitable material for aerobic bacteria containing *nahAc* and that they may persist in capping material for prolonged periods of time. This does not directly correspond to greater potential for biotransformation, but it does indicate a greater presence of gram-negative bacteria capable of naphthalene biodegradation via the *nahAc* dioxygenase gene. The copy numbers of *nahAc* gene decreased more rapidly in microcosms containing organoclay. This was unexpected; active capping materials (organoclay and GAC) are considered to be more likely to retain naphthalene degraders than sand. One possible explanation for asymptotic naphthalene values (Figure 3) and lower *nahAc* copy numbers (Figure 4) in organoclay/oxic microcosms is that organophilic clay may provide bacteria with an alternative carbon source. This would promote biological growth on organoclay (total DNA extracted from organoclay was comparable with the quantity extracted from GAC; Table A.11-A.13 in the Appendix), but the resulting community would not necessarily carry the functional genes needed for naphthalene degradation. This would also consume O_2, potentially explaining asymptotic naphthalene values.

The copy numbers of *nahAc* decreased over the 100-day experiment in anaerobic systems, as shown in Figure 4. This was expected, since the *nahAc* gene is a dioxygenase gene that requires oxygen molecules for ring cleavage, and this gene was likely lost as the microbial community adapted to the anaerobic environment. Nitrate microcosms showed a general trend of decreasing *nahAc* copy numbers over time. The exception was Day 70 for GAC/nitrate microcosms, which showed a spike in *nahAc*, and this was initially attributed to possible trace oxygen within the microcosm. However, spikes in *nahAc* have been observed in additional attempts to enrich nitrate reducers in the presence of naphthalene (data not shown), even though subsequent enrichments were purged extensively with N_2, and careful attention was taken to ensure no accidental O_2 contamination.

CHAPTER IV

DISCUSSION

Role of biodegradation in the decrease of naphthalene concentration

This study monitored and compared naphthalene degradation kinetics in the presence of different capping materials and examined the extent of naphthalene biodegradation under different electron accepting conditions. Decrease of naphthalene concentrations in oxic the experimental microcosms, compared to sterile controls, showed naphthalene losses that could not be explained by adsorption to capping material. Losses were quantified through the evaluation of reaction rate constants.

Decay of naphthalene in sterile controls.

Decrease of naphthalene concentrations was observed in all autoclaved microcosms. It is reasonable to assume that losses through the experimental system observed in the control experiments containing only water and naphthalene, also contributed to naphthalene decreases in sterile microcosms. Nevertheless, the first order decay constants ($k_{observed}$) for autoclaved microcosms were higher than observed first order rate constant ($k_{control}$) for the controls containing only water and naphthalene (Table 1). This suggests the presence of other processes causing naphthalene depletion.

Additional slow adsorption processes on sediment slurries were considered as potential cause of this discrepancy. The microcosms were inoculated with enrichment cultures containing soil particles and dissolved organic carbon following the equilibration period. The equation used to estimate the total mass of naphthalene necessary to reach target concentration at equilibrium, did not account for these matrices. Supplementary adsorption experiments would be necessaries to investigate the potential role of partitioning onto slurry enrichments in naphthalene decrease.

Another likely explanation may be inefficient sterilization of the enriched culture resulting in residual biological activity, as observed in a previous study (Smith

et al., 2006). The survival of soil microorganisms after three cycles of autoclave is not uncommon, particularly when the soil is dissolved in a slurry and not dispersed in a thin layer, as reported by Trevors J.T. in 1996. The *nacAc* copy numbers is sustained for autoclaved microcosms that showed naphthalene decay, such as GAC-oxic systems (Table A.11-A.13 in the Appendix). This supports the hypothesis of incomplete sterilization causing naphthalene decreases in sterile microcosms.

Anaerobic microcosms.

Naphthalene concentrations in microcosms amended with nitrate, sulfate or iron decreased less than 20% when compared to the respective autoclaved controls (Table A.6-A.8 in the Appendix). Nitrate-GAC microcosms exhibited some naphthalene decrease (30 to 50%) within Day 14 and Day 70 samplings (Figure 3-B1), but the trend was not well defined (Figure 3-B2). Biotransformation kinetics under anaerobic conditions are often slow and observation times needed to definitively quantify naphthalene degradation can require few months to years in laboratory microcosms (Rockne et al. 2001, Kummel et al. 2016, and Anderson et al. 2009). Therefore, the process, even if occurring, was not measurable throughout the observation time of these experiments. This can explain the low decreases and the asymptotic behavior of naphthalene concentrations in anaerobic microcosms.

The decay rate constants observed for the GAC and sand anaerobic systems are slightly higher than the ones measured in the control experiments ($0.0165\ day^{-1}$ in GAC sulfate > $k_{observed}$ > $0.0110\ day^{-1}$ for sterile iron sand compared to $k_{control} = 0.0098\ day^{-1}$) for both autoclaved and experimental microcosms (Table 1). A decay constant ($k_{observed}$) greater than $k_{control}$ indicates the presence of additional processes involved in naphthalene depletion. The observed decay constants estimated for experimental microcosms were normalized to the decay constants calculated for respective autoclaved controls (Table 3).

Table 3: Normalized decay constants.

	Ratio $k_{experimental}/k_{autoclaved}$				
	No e-	**Oxygen**	**Nitrate**	**Iron**	**Sulfate**
GAC	1.11	**4.17**	1.38	1.05	1.06
Sand	0.91	1.14	0.99	1.12	1.11

Heat map legend	
	< 0.95
	0.95 - 1.05
	1.05 - 1.15
	1.15 - 1.50
	> 1.5

The ratios between $k_{experimental}$ and $k_{autoclaved}$ is close to 1 for anaerobic microcosms, with the exception of nitrate amended GAC system. The presence of facultative aerobes able to use nitrate as electron acceptors may explain highest naphthalene decay rates in these microcosms. However, as stated previously, the hypothesis of a microaerophilic environment in the anaerobic microcosms is possible due to repeated sampling of serum bottles via syringe, potentially causing oxygen leaking into the systems. In that case, aerobic biotransformation could have occurred contributing to uniform decay of naphthalene in microaerophilic-anaerobic microcosms.

Aerobic microcosms.

Naphthalene concentrations decreased quickly under aerobic conditions (% of naphthalene decreased > 20% compared to respective sterile controls at Day 14 for GAC and sand) and the highest reduction was observed in sediment-cap systems containing activated carbon (concentration in experimental samples was 1% of the autoclaved microcosms at Day 70). The decay of naphthalene can be clearly identified for GAC time series (Figure 3). The calculated first order decay rate constant and the statistical analysis confirmed that naphthalene biotransformation in the presence of GAC is significantly higher than in autoclaved microcosms (Table 3) and water controls ($k_{observed}$ =0.0604 day^{-1} compared to $k_{control}$ = 0.0098 day^{-1}, Table 1). This study suggests that activated carbon is the most efficient and effective of the capping materials studied to support biodegradation of naphthalene in laboratory sediment-cap microcosms. This finding is likely the result of interactions between the material and the microbial community enriched from the contaminated sediments.

Naphthalene decay was also observed in microcosms containing organoclay and sand. However, these time series do not exhibit continuous decreases, and the trend is mostly uniform across the incubation time. The kinetic rate constants estimated for sand and organoclay were not significantly higher than sterilized controls (sand) or not sustained beyond an initial decrease (organoclay). The statistical analysis showed no significance for the $k_{observed}$ values obtained for sand in aerobic conditions (p-values > 0.05). The trend observed in the organoclay microcosms was unexpected. Field data reported appreciable mass flow reduction within organoclay based capping (personal communication with consulting firm Haley and Aldrich). The data collected in this study assess an initial mass reduction of naphthalene in agreement with the field observations, but comparison between the organoclay microcosms and the relative controls shows no improvement. A recent study also proved that the biodegradation of low molecular weight PAHs appears to be neither stimulated nor inhibited in presence of different organoclays (Ugochukwu and Fialips, 2017).

The *nahAc* gene as predictor of naphthalene biodegradation

Biological activity was monitored through quantification of the *nahAc* gene. The plasmids encoding the gene of the naphthalene degradation pathway were first identified in 1982 (Connors and Barnsley., 1982). The plasmid NAH7 containing the *nahAc* gene can be transmitted through duplication (vertical transfer) or conjugation (horizontal transfer). Recent findings demonstrated that the NAH7 plasmid contains transposon sequences able to direct the insertion of the *nahAc* gene in the genomic DNA (Sota M. et al., 2006). Therefore, it is not clear if an increase of the abundance of the *nahAc* gene is proportional to an increase in biomass, which would indicate vertical transfer, or an increase in conjugation frequency (indicating horizontal transfer). The experimental hypothesis was that the gene copy numbers would increase with the population of microorganisms and the percentage of naphthalene biodegraded.

Aerobic microcosms.

The *nahAc* gene abundance increased in presence of sand and activated carbon for oxic systems, as reported in Figure 4. The gene copy numbers spiked in the first two weeks of incubation and then moderately decreased. A previous study that characterized the growth of several naphthalene degrading species, reported that 80% of the biodegradation occurred in the first week, within the transition from lag to log growth phases (Hassanshahian M. et al. 2016). This could explain the initial high abundance of the *nahAc* gene, followed by a decrease that may be related to the microbial communities transitioning into the asymptotic-death phase of growth. The gene abundance would follow growth curve trend if the *nahAc* is associated with either the plasmid or the genome of the microorganism.

However, since the presence of naphthalene is necessary for the bacteria to retain the plasmid, the decrease of gene copy number abundance could be correlated to a decrease of naphthalene concentration during the incubation time. Microcosms were spiked with similar masses of naphthalene (Table 2), but most of the total mass was sequestered onto the adsorbent. The bio-available mass of naphthalene in the systems was in aqueous phase, and measurements of naphthalene concentration were used to study the relationship within substrate abundance and gene transmission. Gene copy numbers were plotted against the mass of naphthalene in solution versus the (Figure 5).

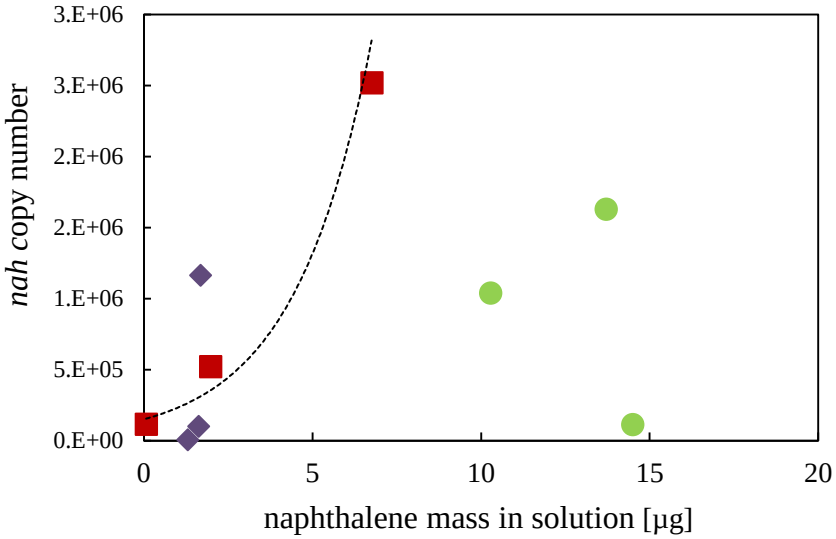

Figure 5: Gene abundance versus mass of naphthalene in solution. Here reported microcosms prepared with GAC (■), organoclay (◆) and sand (●).

The naphthalene decay in sand and organoclay systems was not consistent, and the gene copy numbers decreased after an initial spike. The mass of naphthalene in solution did not show any correlation with gene concentration in sand microcosms. Organoclay data points presented very low correlation ($R^2 < 0.5$) when fitted with an exponential or linear regression. Therefore, the relationship between decreases of gene abundance and mass of naphthalene is not evident in oxic organoclay microcosms. This is consistent with the hypothesis that the presence of organoclay does not affect the biodegradation of naphthalene mentioned in the previous section.

The mass of naphthalene in solution and gene copy numbers followed a defined trend in activated carbon systems. The dashed line represents an exponential curve fitted to the experimental data ($R^2 = 0.948466$). These preliminary results suggest that a correlation between mass of naphthalene in solution and gene abundance exists in the presence of GAC, although additional data points are needed to confirm it.

Anaerobic microcosms.

The *nahAc* gene, indicating the presence of oxic naphthalene degraders, has been well documented, but a similar anaerobic biomarker does not exist. A recently developed method for detecting the naphthalene degradation gene *ncr*, present under sulfate conditions, shows promise, but (to the best of our knowledge) has only been tested using liquid enrichments, not sediment systems, and is in elementary stages of development (Morris et al., 2014 and von Netzer F. et al., 2016). This new biomarker assay for *ncr* is not well understood, is specific to sulfate-reducing *Deltaproteobacteria*, and it is unknown whether *dhncr* genes (a naphthalene degradation gene distinct from *ncr*) would be detected using the *ncr* assay. In absence of a biomarker, qPCR is not an appropriate analysis for these microcosms. Instead, cultures that demonstrate degradation of naphthalene under anoxic conditions can be sequenced, to compare microbial community members within microcosm samples to known sulfate-reducing consortia.

However, microcosm experiments did not yield data indicating transformation of naphthalene under anaerobic conditions, likely due to insufficient experimental timeframes (Kummel et al., 2016).For this reason community analysis have been postponed.

Relationship between capping material type and biodegradation

The goal of this study was to investigate the correlation between capping material and biodegradation activity in laboratory microcosms resembling in situ conditions. The experimental hypothesis was that the type of capping material used affected the growth and development of the native microbial communities, including those species able to metabolize naphthalene. The findings of this study suggest that activated carbon supports the biodegradation of naphthalene under aerobic conditions. Sediment-cap microcosms containing GAC showed stable continuous decrease of naphthalene concentrations and sustained gene copy numbers across the observation

time. Moreover, the presence of GAC appeared to be associated with the correlation between abundance of catabolic genes and residual mass of naphthalene in solution.

The hypothesis of the development of a biofilm on the surface area of the activated carbon can justify these findings. The suitability of GAC to support high growth of biomass in a biofilm matrix has been reported in previous studies in both drinking water and wastewater treatment (Edwards S.J., 2013). The overall cellular uptake of PAHs improved in presence of biofilms, due to facilitate adsorption and transport within the biofilm matrix (Johnsen and Karlson 2004). This increased availability of naphthalene can enhance positive feedback within the cells, leading to replication and transmission of the plasmid. In addition, biofilm growth is often associated with high frequency of horizontal transfer, in other words increase of bacterial conjugation (Martirani et al., 2017). These two mechanisms, characteristics of biofilm growth, can ultimately increase the abundance of the *nahAc* gene with respect to high naphthalene concentrations when GAC is present.

In addition, the physical proximity within the biofilm matrix can lead to the development of a consortium where synergy and co-metabolism enhance the biodegradation capability of the system (Heidler and Halden 2007; Lolas et al. 2012). While fascinating, further investigations are necessary to prove this hypothesis.

CHAPTER V

CONCLUSION

This study investigated the effects of different capping materials upon the biodegradation of a model PAH in laboratory microcosms. The decay of naphthalene due to biological activity and the abundance of a biomarker, the naphthalene dioxygenase gene, were monitored in laboratory microcosms resembling sediment cap environments. The experiments tested three different capping materials (sand, organoclay and activated carbon) and four electron acceptors (oxygen, nitrate, sulfate and iron hydroxide).

The results showed that naphthalene concentration decreases only in oxic sediment-cap systems during the observation time. The naphthalene decay was statistically significant in oxic microcosms prepared with activated carbon only. This result suggests that activated carbon was the most efficient of the capping materials tested.

The data collected were modeled without accounting for potential desorption of naphthalene from capping material. Consequently, the observed kinetics might be significantly underestimated due to the low percentage of naphthalene in aqueous phase with respect to the total masses in the systems.

Abundance of the *nahAc* gene was sustained in oxic microcosms prepared with GAC and sand. The selected biomarker should not have been detected in anaerobic microcosms, but microaerophilic environments could have led to viable aerobic cultures. The *nahAc* gene was a good predictor of naphthalene degradation in aerobic sediment-cap microcosms.

Within oxic sediment-cap systems, a relationship between the naphthalene mass in solution and the gene copy numbers was observed in the microcosms prepared with activated carbon. This suggests that the nature of the capping material affected the

interaction between abundance of the catabolic gene and concentration of the substrate (naphthalene).

The relationship between capping material and biodegradation activity needs to be further investigated. This study was intended to screen a matrix of variables, and for this reason, the time courses consisted of three biomarker sampling points only. A more detailed microcosm study under aerobic conditions, with extended samplings, would provide additional data and improve the statistical significance of our findings. Furthermore, the use of community analysis would led to identify changes of the microbial community in the presence of capping materials.

Additional studies are currently underway to better understand how capping materials can affect PAH biodegradation under anaerobic conditions over longer periods of time. The sediment environment is mostly anoxic (< 2 mg/L O_2) or anaerobic (~0 mg/L O_2). Beneath a superficial aerobic layer, sediments consist of a gradient of different redox zones, stratified according to the biogeochemical processes occurring and the redox potential of the terminal electron acceptors. Each redox zone is characterized by a niche of microorganisms adapted to those specific conditions (Himmelheber et al., 2009). In contaminated sites, anaerobic niches are likely to contain microorganisms able to degrade the pollutants. A capping material that sustain and stimulate the growth of microbial communities under anaerobic conditions, could greatly improve biodegradation within a bio-reactive capping system.

To our knowledge, this work is the first to suggest that capping media selection significantly influences biodegradation of PAHs within sediment caps. These initial findings suggest that correct media selection during capping design can be critical in sustaining biodegradation activity. Therefore, the concept of a bio-reactive cap is feasible. The selection of a capping material that sustains and promotes biodegradation is the first step in designing a capping system that not only preserves the environment from contamination, but also enhance degradation of the pollutants. The reduction of the mass of contaminants within the capping system, reduces the risk of exposure in

case of leaks, aging or extraordinary circumstances like the erosion of the capping during tropical storms and hurricanes. Ultimately, the concept behind the design of a bio-reactive capping is moving the remediation target from the containment of the risk, towards the efficient conversion of the contaminants into benign products.

BIBLIOGRAPHY

U.S. EPA. Health Effects Assessment for Polycyclic Aromatic Hydrocarbons (PAHs). Washington, DC: U.S. Environmental Protection Agency, EPA /540/1-86/013 (NTIS PB86134244), 1984.

Abdel-Shafy H.I. and Mansour M.S.M. A review on polycyclic aromatic hydrocarbons: Source, environmental impact, effect on human health and remediation. Egyptian Journal of Petroleum, 2016.

Anderson R.T. and Lovley D.R. Naphthalene and Benzene Degradation under Fe (III)-Reducing Conditions in Petroleum-Contaminated Aquifers. Bioremediation Journal 2009.

Baldwin B.R., Nakatsub C.H. and Niesa L. Enumeration of aromatic oxygenase genes to evaluate monitored natural attenuation at gasoline-contaminated sites. Water research, 2008.

Baker H.M., Massadeh A.M. and Younes H.A. Natural Jordanian zeolite: removal of heavy metal ions from water samples using column and batch methods. Environmental monitoring and assessment, 2009.

Borisover M., Bukhanovsky N., Lapides I. and Yariv S. Thermal treatment of organoclays: effect on the aqueous sorption of nitrobenzene on n-hexadecyltrimethyl ammonium montmorillonite. Applied Surface Science, 2010.

Carmona M., Zamarro M.T., Blazques B., Durante-Rodríguez G., Juarez J.F., Valderrama J.A., Barragan M.J.L., García J.L. and Díaz E. Anaerobic catabolism of aromatic compounds: a genetic and genomic view. Microbiology and molecular biology reviews, 2009.

Cebron A., Norini M.P., Beguiristain T. and Leyval C. Real-Time PCR quantification of PAH-ring hydroxylating dioxygenase (PAH-RHDα) genes from Gram positive and Gram negative bacteria in soil and sediment samples. Journal of Microbial Methods, 2008.

Connors M.A. and Barnsley E.A. Naphthalene Plasmids in Pseudomonads. Journal of Bacteriology, 1982.

Dunlap P. J. Thesis. The University of Texas at Austin, 2011.

Edwards S.J. and Kjellerup B.V. Applications of biofilms in bioremediation and biotransformation of persistent organic pollutants, pharmaceuticals/personal

care products, and heavy metals. Applied Microbiology and Biotechnology, 2013.

Erdem et al. 2004; Erdem E, Karapinar N, Donat R (2004) The removal of heavy metal cations by natural zeolites. J Colloid Interface Sci

Eriksson M., Sodersten E., Yu Z., Dalhammar G. and Mohn W.W. Degradation of Polycyclic Aromatic Hydrocarbons at Low Temperature under Aerobic and Nitrate-Reducing Conditions in Enrichment Cultures from Northern Soils. Applied and Environmental Microbiology, 2003.

Foght J. Anaerobic Biodegradation of aromatic hydrocarbons: pathways and prospects. Journal of molecular microbiology and biotechnology, 2008.

Gilmour C.C., Riedel G.S., Riedel G., Kwon S., Landis R., Brown S.S., Menzie C.A. and Ghosh U. Activated carbon mitigates mercury and methylmercury bioavailability in contaminated sediments. Environmental Science and Technology, 2013.

Hassanshahian M. and Boroujeni N.A. Enrichment and identification of naphthalene-degrading bacteria from the Persian Gulf. Marine Pollution Bulletin, 2016.

Hamidpour M., Kalbasi M., Afyuni M., Shariatmadari H., Holm P.E. and Hansen H.C.B. (2010) Sorption hysteresis of Cd (II) and Pb (II) on natural zeolite and bentonite. Journal of hazardous materials, 2010.

Heidler J. and Halden R.U. Mass balance assessment of triclosan removal during conventional sewage treatment. Chemosphere, 2007.

Himmelheber D.W., Thomas S.H., Loffler F.E., Taillefert M. and Hughes J.B. Microbial colonization of an in situ sediment cap and correlation to stratified redox zones. Environmental science and technology, 2009.

Himmelheber D.W, Pennell K.D. and Hughes J.B.Evaluation of a laboratory-scale bioreactive in situ sediment cap for the treatment of organic contaminants. Water Research, 2011.

Hyun S., Jafvert C.T., Lee L.S. and Rao P.S.C. Laboratory studies to characterize the efficacy of sand capping a coal tar-contaminated sediment. Chemosphere, 2006.

Johnsen A.R. and Karlson U. Evaluation of bacterial strategies to promote the bioavailability of polycyclic aromatic hydrocarbons. Applied Microbiology and Biotechnology, 2004.

Kanel S.R., Manning B., Charlet L. and Choi H. Removal of arsenic (III) from groundwater by nanoscale zero-valent iron. Environmental science and technology, 2005.

Kim Y.S., Leila M. Nyberg L.M., Jenkinson B. and Jafvert C.T. PAH concentration gradients and fluxes through sand cap test cells installed in situ over river sediments containing coal tar. Environmental science processes & impacts, 2013.

Kwon M.J. and Finneran K.T. Hexahydro-1,3,5-trinitro-1,3,5-triazine (RDX) and Octahydro-1,3,5,7-tetranitro-1,3,5,7-tetrazocine (HMX) Biodegradation Kinetics Amongst Several Fe(III)-Reducing Genera. Journal of Soil and Sediment Contamination: An International Journal, 2008

Kržišnik N., Mladenovič A., Škapin A.S., Škrlep L., Ščančar J. and Milačič R. Nanoscale zero-valent iron for the removal of Zn2+, Zn (II)– EDTA and Zn (II)–citrate from aqueous solutions. Science of total environment, 2014.

Kummel S., Herbst F.A., Bahr A., Duarte M., Pieper D.H., Jehmlich N., Seifert J., von Bergen M., Bombach P., Richnow H.H. and Vogt C. Anaerobic naphthalene degradation by sulfate reducing Desulfobacteraceae from various anoxic aquifers. FEMS 2015.

Lolas I.B., Chen X., Bester K. and Nielsen J.L. Identification of triclosan-degrading bacteria using stable isotope probing, fluorescence in situ hybridization and micro autoradiography. Microbiology, 2012.

Mahabadi A.A., Hajabbasi M., Khademi H. and Kazemian H. Soil cadmium stabilization using an Iranian natural zeolite. Geoderma, 2007.

Martirani-Von Abercron S.M., Marin P., Solsona-Ferraz,M., Castaneda-catana M.A. and Marques S. Naphthalene biodegradation under oxygen-limiting conditions: community dynamics and the relevance of biofilm-forming capacity. Microbial biotechnology, 2017.

Millward R.N., Bridges T.S., Ghosh U., Zimmerman J.R., Luthy R.G. Addition of activated carbon to sediments to reduce PCB bioaccumulation by a polychaete (Neanthes arenaceodentata) and an amphipod (Leptocheirus plumulosus). Environmental Science and Technology, 2005.

Montgomery J.H. and Welkom L.M. Groundwater chemicals desk reference. Lewis, 1990.

Morris B.E.L., Gissibl A., Kummel S., Richnow H.H. and Boll M. A PCR-based assay for the detection of anaerobic naphthalene degradation. FEMS Microbiology Letters, 2014.

Murphy P., Marquette A., Reible D. and Lowry G.V. Predicting the performance of activated carbon-, coke-, and soil-amended thin layer sediment caps. Journal of Environmental Engineering, 2006.

Nyyssonen M., Piskonen R. and Itavaaran M. Monitoring aromatic hydrocarbon biodegradation by functional marker genes. Environmental pollution, 2008.

Park J.W. and Crowley D.E. Dynamic changes in nahAc gene copy numbers during degradation of naphthalene in PAH-contaminated soils. Applied microbiology and biotechnology 2006.

Park Y., Ayoko G.A. and Frost R.L. Application of organoclays for the adsorption of recalcitrant organic molecules from aqueous media. Journal of Colloid Interface Science, 2011.

Peng R., Xiong A., Xue Y., Fu X., Gao F., Zhao W., Tian Y. and Yao Q. Microbial biodegradation of polyaromatic hydrocarbons. FEMS Microbiology Review, 2008.

Petersen E.J., Pinto R.A., Shi X. and Huang Q. Impact of size and sorption on degradation of trichloroethylene and polychlorinated biphenyls by nano-scale zerovalent iron. Journal of hazardous materials, 2012.

Reible D., Processes, Assessment and Remediation of Contaminated Sediments. SERDP ESTCP Environmental Remediation Technology, Springer, 2014.

Reible D., Lampert D., Constant D., Mutch R.D. and Zhu Y. Active Capping Demonstration in the Anacostia River, Washington, D.C. Remediation, 2006.

Rockne K.J. and Strand S.E. Anaerobic biodegradation of naphthalene, phenanthrene, and biphenyl by a denitrifying enrichment culture. Water Research 2001.

Sarkar B., Megharaj M., Shanmuganathan D. and Naidu R. Toxicity of organoclays to microbial processes and earthworm survival in soils. Journal of Hazard Materials, 2012.

Seo J.S., Keum Y.S. and Li Q.X. Bacterial Degradation of Aromatic Compounds. Journal of Environmental Research and Public Health, 2009.

Smith A., Kirisits M.J. and Reible D. Assessment of potential anaerobic biotransformation of organic pollutants in sediment caps. New Biotechnology, 2012

Sota M., Yano H., Ono A., Miyazaki R., Ishii H., Genka H., Top E.M. and Tsuda M. Genomic and functional analysis of the incp-9 naphthalene-catabolic plasmid nah7 and its transposon tn4655 suggests catabolic gene spread by a tyrosine recombinase. Journal of Bacteriology, 2006.

Trevors J. T. Sterilization and inhibition of microbial activity 1n soil. Journal of Microbiological Methods 26 (1996) 53-59

Ugochukwu U.C. and Fialips C.I. Removal of crude oil polycyclic aromatic hydrocarbons via organoclay-microbe-oil interactions. Chemosphere, 2017.

Vogt C., Gödeke S., Treutler H.C., Weiß H., Schirmer M. and Richnow H.H.Benzene oxidation under sulfate-reducing conditions in columns simulating in situ conditions. Biodegradation, 2007.

von Netzer F., Kuntze K., Vogt C., Richnow H.H., Boll M. and Lueders T.(2016) Functional gene markers for fumarate-adding and dearomatizing key enzymes in anaerobic aromatic hydrocarbon degradation in terrestrial environments. Journal of Molecular Microbiology and Biotechnology, 2016.

Werner D., Higgins C.P., Luthy R.G. The sequestration of PCBs in Lake Hartwell sediment with activated carbon.Water Research, 2005.

Wingenfelder U., Hansen C., Furrer G. and Schulin R. Removal of heavy metals from mine waters by natural zeolites. Environmental science and technology, 2005.

Yan F. and Reible D. Electro-bioremediation of contaminated sediment by electrode enhanced capping. Journal of Environmental Management, 2015.

APPENDIX

Table A. 1: Composition of GAC microcosms containing.

Sample Series		GAC [mg]	Porewater [mL]	Inoculum [mL]	Media [mL]	Buffer [mL]	Acceptor [mL]	Naphthalene* [µL]
No Acceptor	Autoclaved (Sterile)	5	3	1.5	19.875	0.625	0	20
	Experimental	5	3	1.5	19.875	0.625	0	20
Oxygen	Autoclaved (Sterile)	5	3	1.5	19.875	0.625	0	20
	No Naphthalene	5	3	1.5	19.875	0.625	0	0
	Experimental	5	3	1.5	19.875	0.625	0	20
Nitrate	Autoclaved (Sterile)	5	3	1.5	19.625	0.625	0.25	20
	No Naphthalene	5	3	1.5	19.625	0.625	0.25	0
	Experimental	5	3	1.5	19.625	0.625	0.25	20
Sulfate	Autoclaved (Sterile)	5	3	1.5	19.625	0.625	0.25	20
	No Naphthalene	5	3	1.5	19.625	0.625	0.25	0
	Experimental	5	3	1.5	19.625	0.625	0.25	20
Iron	Autoclaved (Sterile)	5	3	1.5	19.375	0.625	0.5	20
	No Naphthalene	5	3	1.5	19.375	0.625	0.5	0
	Experimental	5	3	1.5	19.375	0.625	0.5	20

Table A. 2: Composition of organoclay microcosms.

Sample Series		Organo clay [mg]	Porewater [mL]	Inoculum [mL]	Media [mL]	Buffer [mL]	Acceptor [mL]	Naphthalene* [µL]
No Acceptor	Autoclaved (Sterile)	668	3	1.5	19.875	0.625	0	20
	Experimental	668	3	1.5	19.875	0.625	0	20
Oxygen	Autoclaved (Sterile)	668	3	1.5	19.875	0.625	0	20
	No Naphthalene	668	3	1.5	19.875	0.625	0	0
	Experimental	668	3	1.5	19.875	0.625	0	20
Nitrate	Autoclaved (Sterile)	668	3	1.5	19.625	0.625	0.25	20
	No Naphthalene	668	3	1.5	19.625	0.625	0.25	0
	Experimental	668	3	1.5	19.625	0.625	0.25	20
Sulfate	Autoclaved (Sterile)	668	3	1.5	19.625	0.625	0.25	20
	No Naphthalene	668	3	1.5	19.625	0.625	0.25	0
	Experimental	668	3	1.5	19.625	0.625	0.25	20
Iron	Autoclaved (Sterile)	668	3	1.5	19.375	0.625	0.5	20
	No Naphthalene	668	3	1.5	19.375	0.625	0.5	0
	Experimental	668	3	1.5	19.375	0.625	0.5	20

Table A. 3: Composition of sand microcosms.

Sample Series		Sand [mg]	Porewater [mL]	Inoculum [mL]	Media [mL]	Buffer [mL]	Acceptor [mL]	Naphthalene* [µL]
No Acceptor	Autoclaved (Sterile)	668	3	1.5	19.875	0.625	0	20
	Experimental	668	3	1.5	19.875	0.625	0	20
Oxygen	Autoclaved (Sterile)	668	3	1.5	19.875	0.625	0	20
	No Naphthalene	668	3	1.5	19.875	0.625	0	0
	Experimental	668	3	1.5	19.875	0.625	0	20
Nitrate	Autoclaved (Sterile)	668	3	1.5	19.625	0.625	0.25	20
	No Naphthalene	668	3	1.5	19.625	0.625	0.25	0
	Experimental	668	3	1.5	19.625	0.625	0.25	20
Sulfate	Autoclaved (Sterile)	668	3	1.5	19.625	0.625	0.25	20
	No Naphthalene	668	3	1.5	19.625	0.625	0.25	0
	Experimental	668	3	1.5	19.625	0.625	0.25	20
Iron	Autoclaved (Sterile)	668	3	1.5	19.375	0.625	0.5	20
	No Naphthalene	668	3	1.5	19.375	0.625	0.5	0
	Experimental	668	3	1.5	19.375	0.625	0.5	20

*The concentration of the naphthalene stock [in acetonitrile] was 40000 mg/L

Table A. 4: Capping material properties and naphthalene partitioning.

Granular Activated Carbon					
	Water	Air	Capping Material	Dissolved Organic Carbon	
Capping mass, [mg]			5.00		
Volume, [L]	0.025	0.005		0.003	Σ =
Naphthalene mass, [mg]	0.025	0.0001115	0.733	0.0003	0.7584 mg
Organoclay Diameter = 0.000002 m, density = 800.92 g/L, approximate volume occupied = 0.835 mL in microcosms					
	Water	Air	Capping Material	Dissolved Organic Carbon	
Capping mass, [mg]			668.6		
Volume, [L]	0.025	0.005		0.003	Σ =
Naphthalene mass, [mg]	0.025	0.0001115	0.733	0.0003	0.7584 mg
Sand Diameter = 0.00005 m, density = 1602 g/L, approximate volume occupied = 4.17 mL in microcosms					
	Water	Air	Capping Material	Dissolved Organic Carbon	
Capping mass, [mg]			6685.74		
Volume, [L]	0.025	0.005		0.003	Σ =
Naphthalene mass, [mg]	0.025	0.0001115	0.733	0.0003	0.7584 mg
Sediments					
	Water	Air	Capping Material	Dissolved Organic Carbon	
Capping mass, [mg]			5000		
Volume, [L]	0.025	0.005		0.025	Σ =
Naphthalene mass, [mg]	0.025	0.0001115	0.151	0.025	0.1760 mg

Standard curve for quantification of *nahAc* gene

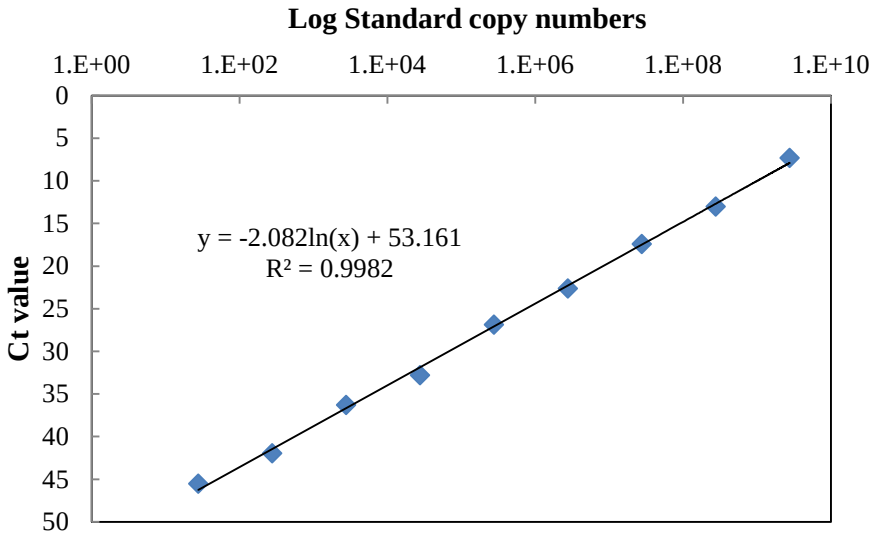

Figure A. 1: Standards curve used to quantify the *nahAc* gene.

The *nahAc* gene, from *Pseudomonas putida* 9816-4 has GenBank # [AF491307] (http://www.ncbi.nlm.nih.gov/nuccore/AF491307).

The primers used are the PAH-RHDα GN (Cebron et al., 2008):

GAGATCCATACCACGTKGGTTGGA [forward]

AGCTGTTGTTCGGGAAGAYWGTGCMGTT [reverse]

Below reported the sequence of the 306 bp amplicon, and the sections underlined mark primer binding locations.

gagatgcata ccacgtgggt tggacgcacg cgtcttcgct tcgctcgggg
gagtctatct tctcgtcgct cgctggcaat gcggcgctac cacctgaagg
cgcaggcttg caaatgacct ccaaatacgg cagcggcatg ggtgtgttgt
gggacggata ttcaggtgtg catagcgcag acttggttcc ggaattgatg
gcattcggag gcgcaaagca ggaaaggctg aacaaagaaa ttggcgatgt
tcgcgctcgg atttatcgca gccacctcaa ctgcaccgtt ttcccgaaca acagca

Standards utilized for this study include the amplicon, plus an additional 10 base pairs on either end; the sequence utilized for standards (326 bp) is:

aactttgtgg gagatgcata ccacgtgggt tggacgcacg cgtcttcgct
tcgctcgggg gagtctatct tctcgtcgct cgctggcaat gcggcgctac
cacctgaagg cgcaggcttg caaatgacct ccaaatacgg cagcggcatg
ggtgtgttgt gggacggata ttcaggtgtg catagcgcag acttggttcc
ggaattgatg gcattcggag gcgcaaagca ggaaaggctg aacaaagaaa
ttggcgatgt tcgcgctcgg atttatcgca gccacctcaa ctgcaccgtt
ttcccgaaca acagcatgct gacctg

Table A. 5: PAH concentrations in bulk sediment.

PAH	Elution Time [min]	Concentration [µg/kg]	Standard Deviation
NAP	8.116	10475.45	2123.9
FL	11.308	1771.31	1050.9
ACE	11.729	3544.48	1989.1
PHE	12.347	6085.13	3880.9
ANT	13.183	1723.99	943.0
FLU	15.375	2298.99	868.3
PYR	16.619	3145.77	1294.3
CHR	20.95	617.81	24.5
BaA	21.902	929.32	78.4
BbF	27.004	536.73	207.6
BkF	28.183	277.89	30.6
BaP	29.487	949.98	129.0
DBA	37.804	81.09	9.4
Inp + BghiP	39.653	693.35	92.3

Table A. 6: Aqueous naphthalene concentrations in GAC microcosms.

Sample Series		Aqueous Concentration of Naphthalene (ppb)					
		Baseline	**14 days**	**35 days**	**56 days**	**70 days**	**100 days**
No Acceptor	**Autoclaved (Sterile)**	1180.26	771.98	471.84			
		1207.08	636.17	395.51	393.02	355.95	
		1126.61	650.47	444.08	393.02	341.11	353.20
	Experimental	599.07	328.81	222.04			
		760.01	493.21	312.24	289.21	229.88	
		956.72	2.36	326.12	318.87	259.54	253.38
Oxygen	**Autoclaved (Sterile)**	706.37	89.53				
		ND	ND	ND			
		974.61	593.82	430.20	437.52	370.78	
	Experimental	348.71	137.04				
		304.01	584.68	90.20			
		232.47	88.62	67.31	63.77	2.52	
Nitrate	**Autoclaved (Sterile)**	1376.97	841.28	568.98			
		849.43	343.75	242.86	511.67	444.93	
		1207.08	578.95	374.69	385.61	326.28	268.74
	Experimental	929.90	551.81	367.75			
		500.72	289.47	208.16	163.14	155.73	
		688.48	280.43	249.80	237.30	192.80	199.64
Sulfate	**Autoclaved (Sterile)**	715.31	520.41	340.00			
		1072.96	610.61	346.94	348.53	296.62	
		1072.96	562.04	395.51	393.02	318.87	299.45
	Experimental	625.89	353.88	222.04			
		992.49	548.16	367.75	341.11	304.04	
		1207.08	659.18	367.75	393.02	326.28	261.06
Iron	**Autoclaved (Sterile)**	1806.15	222.04	686.94			
		1430.62	ND	686.94	615.49	541.33	
		1770.39	1200.41	652.24	659.98	400.44	406.95
	Experimental	1922.389	1304.49	652.24			
		1797.21	1269.79	673.06	689.64	533.92	
		1600.501	1040.82	673.06	578.41	467.18	376.24

Table A. 7: Aqueous naphthalene concentrations in organoclay microcosms.

Sample Series		Aqueous Concentration of Naphthalene (ppb)					
		Baseline	**14 days**	**35 days**	**56 days**	**70 days**	**100 days**
No Acceptor	**Autoclaved (Sterile)**	702.23	157.26	140.90			
		510.72	114.37	103.82	111.23	106.78	
		738.71	157.26	163.14	163.14	137.29	122.85
	Experimental	702.23	142.96	103.82			
		756.95	171.55	148.31	170.56	144.92	
		793.43	164.40	133.48	148.31	137.29	99.82
Oxygen	**Autoclaved (Sterile)**	938.82	155.31				
		884.13	173.58	148.31			
		683.61	164.44	155.73	177.97	160.17	
	Experimental	55.60	70.34				
		54.69	73.09	72.67			
		13.67	57.55	57.10	55.62	51.87	
Nitrate	**Autoclaved (Sterile)**	802.55	226.15	185.39			
		647.51	217.11	163.14	185.39	175.43	
		647.51	208.06	170.56	177.97	175.43	176.60
	Experimental	1203.83	226.15	163.14			
		1240.31	208.06	170.56	177.97	137.29	
		1121.75	208.06	140.90	177.97	160.17	176.60
Sulfate	**Autoclaved (Sterile)**	501.60	111.02	140.90			
		766.07	152.65	96.40	103.82	129.66	
		638.39	117.96	103.82	111.23	106.78	73.71
	Experimental	966.71	90.20	163.14			
		1057.91	194.29	155.73	207.64	175.43	
		747.83	145.71	296.62	118.65	114.41	92.14
Iron	**Autoclaved (Sterile)**	994.07	263.67	296.62			
		829.91	215.10	126.06	118.65	122.04	
		1057.91	228.98	126.06	155.73	144.92	115.17
	Experimental	1121.12	270.61	148.31			
		1184.92	277.55	170.56	185.39	160.17	
		975.28	228.98	170.56	133.48	122.04	130.53

Table A. 8: Aqueous naphthalene concentrations in sand microcosms.

Sample Series		Aqueous Concentration of Naphthalene (ppb)					
		Baseline	**14 days**	**35 days**	**56 days**	**70 days**	**100 days**
No Acceptor	**Autoclaved (Sterile)**	4085.55	1679.78	1086.50			
		3171.56	1308.08	850.61	875.03	793.23	
		2778.54	1165.12	757.69	763.80	709.33	514.45
	Experimental	3427.47	1479.64	1029.31			
		2952.20	1343.82	914.94	971.44	823.74	
		3071.02	1343.82	922.09	926.94	808.49	644.98
Oxygen	**Autoclaved (Sterile)**	1837.13	66.69				
		3372.64	1406.90	900.65			
		3162.42	1342.95	907.80	904.70	839.00	
	Experimental	ND	29.23				
		3189.84	255.80	193.00			
		2879.08	840.48	629.02	637.74	579.67	
Nitrate	**Autoclaved (Sterile)**	2997.90	1239.31	793.43			
		3829.63	1438.32	1007.87	1075.25	892.39	
		2778.54	1067.43	686.21	748.97	686.45	545.16
	Experimental	3025.32	61.51	893.50			
		3025.32	1248.35	850.61	860.20	732.22	
		2769.40	ND	872.06	904.70	739.84	568.19
Sulfate	**Autoclaved (Sterile)**	3445.75	1026.94	636.17			
		under LDL	1387.75	843.46	1594.34	800.86	
		3756.51	1609.79	979.28	1067.84	961.03	721.76
	Experimental	3034.46	1401.63	886.35			
		3555.43	1491.84	964.98	1001.10	846.62	
		3061.88	1242.04	786.28	875.03	762.72	614.26
Iron	**Autoclaved (Sterile)**	3464.03	ND	872.06			
		ND	1228.16	714.80	748.97	655.94	
		3409.19	ND	1036.46	1134.58	953.41	729.44
	Experimental	3473.174	1630.61	907.80			
		2266.703	1401.63	814.87	875.03	747.47	
		3628.553	1595.92	814.87	993.68	854.25	783.19

Estimation of uncertainties for function of several independent measurements

The average of the concentrations in autoclaved microcosms is a measurement with uncertainty $\sigma_{C_{control}}$, and the concentration in experimental microcosms at time i normalized by the average of the controls at time i is a function of $C_{Control}$. Given the condition of independency for all the variable, the following relationship holds:

$$\sigma_{C_i} \approx \left|\frac{dC_i}{dC_{Control}}\right| \sigma_{C_{Control}} \textbf{ (10)}$$

$$\sigma_{C_i} \approx \left|\frac{d\left(\frac{C_i}{C_{Control}}\right)}{dC_{Control}}\right| \sigma_{C_{Control}} \approx \left|\frac{C_i}{C_{Control}^2}\right| \sigma_{C_{Control}} \; equation \textbf{ (11)}$$

Average of concentration ratio are reported in Figure 3. Given that all of the measurements are independents, the final error for the average of the concentration ratios is expressed by the equation:

$$\sigma_{C_{average}} \approx \sqrt{\sum_{i=1}^{n=3} \left(\frac{\partial C_{average}}{\partial C_i}\right)^2 \sigma_{C_i}^2} \; eqation \textbf{ (12)}$$

Table A. 9: Aqueous naphthalene concentrations in DDI controls.

date	$C_{naphthalene}$ [µg/L]	Average conc	St.Dev
12.04	2718.12	2477.53	12.54
	2587.59		
	2126.89		
12.18	1604.77	1623.96	1.67
	1643.16		
1.07	1228.53	1246.45	2.49
	1282.28		
	1228.53		
3.16	775.51	819.02	6.91
	883.01		
	798.54		

Table A. 10: Statistics for DDI controls

	Coefficients	***t Stat***	***P-value***	***Lower 95%***	***Upper 95%***
Intercept	7.624176	101.4961	4.44E-15	7.454247	7.794104
Coefficient	-0.00986	-7.21582	5E-05	-0.01294	-0.00677

Table A. 11: DNA concentrations and *nahAc* copy numbers in GAC systems

Sample Series		Day 14		Day 35		Day 70		Day 100	
		DNA[a]	*nahAc*[b]	DNA	*nahAc*	DNA	*nahAc*	DNA	*nahAc*
No Acceptor	**Autoclaved (Sterile)**			36.8	NA	648	NA	15.4	29
					NA		NA		Too Low
	Experimental			924	75,556	514	17,556	25.6	367
					66,305		14,937		333
Oxic	**Autoclaved (Sterile)**	2,960	1,637	5,600	188,229	4880	NA		
			1,262		211,224		NA		
	No naphthalene	2,500	22,628	8,780	3,830	846	3,863		
			20,204		4,642		10,000		
	Experimental	3,400	2,548,484	1,018	594,668	1510	120,610		
			2,492,728		451,961		114,031		
NO_3^{2-}	**Autoclaved (Sterile)**			Too Low	NA	123	14	18.6	Too Low
					NA		NA		NA
	No naphthalene			1,624	1,480	868	1,763	686	213
					1,207		1,797		157
	Experimental			151	35,893	3100	524,474	1472	22,943
					50,606		607,924		20,817
SO_4^{2-}	**Autoclaved (Sterile)**			29.6	33,186	218	87,854	109	3,030
					29,803		77,188		2,548
	No naphthalene			1,064	4,132	346	2,031	56.6	32
					4,040		1,980		70
	Experimental			1,344	339,887	460	19,429	98	
					347,645		23,229		113
Fe^{3+}	**Autoclaved (Sterile)**			784	Too Low	508		Too Low	NA
					39				NA
	No naphthalene			928	2,984	322	6,424	139	263
					3,009		6,727		297
	Experimental			514	20,843	542	21,877	289	3,691
					20,799		23,951		3,012

Table A. 12: DNA concentrations and *nahAc* copy numbers in organoclay systems

Sample Series		Day 14		Day 35		Day 70		Day 100	
		DNA[a]	*nahAc*[b]	DNA	*nahAc*	DNA	*nahAc*	DNA	*nahAc*
No Acceptor	**Autoclaved (Sterile)**			174	928	107	NA	Too Low	NA
					985		NA		NA
					1,320				
	Experimental			558	13,664	340	Too Low	102	336
					21,346		99		450
					19,081				
Oxic	**Autoclaved (Sterile)**	6,200	2,075	8,520	435	2,940	17		
			2,214		365		64		
	No naphthalene	3,380	56,023	5,240	48,743	7,280	2,571		
			60,332		46,037		8,847		
	Experimental	2,880	1,253,911	3,380	126,342	420	7,636		
			1,076,393		76,864		28,914		
NO_3^{2-}	**Autoclaved (Sterile)**			558	73	938	30	Too Low	NA
					80		Too Low		NA
					91				
	No naphthalene			1,170	44,891	2,820	5,931	756	5,646
					32,700		9,739		4,041
					41,833				
	Experimental			816	79,933	3,120	14,264	776	29,774
					115,984		20,894		26,923
SO_4^{2-}	**Autoclaved (Sterile)**			274	Too Low	246	416	12.8	Too Low
					74		536		Too Low
	No naphthalene			1,166	7,448	2,040	10,782	Too Low	1,082
					7,033		16,332		1,039
	Experimental			996	15,321	242	43,303	266	1,165
					22,599		47,706		1,555
					19,193				
Fe^{3+}	**Autoclaved (Sterile)**			294	539	94	213	54.2	Too Low
					375		NA		Too Low
	No naphthalene			496	2,860	1064	68,354	184	1,166
					8,279		76,090		948
	Experimental			572	9,179	111	14,151	328	5,101
					14,916		13,228		5,281
					14,883				

Table A. 13: DNA concentrations and *nahAc* copy numbers in sand systems.

Sample Series		Day 14		Day 35		Day 70		Day 100	
		DNA[a]	*nahAc*[b]	DNA	*nahAc*	DNA	*nahAc*	DNA	*nahAc*
No Acceptor	**Autoclaved (Sterile)**			1,206	355,692	193	17,557	70.6	NA
					310,612		NA		NA
	Experimental			886	14,350	185	8,166	115	873
					24,253		7,737		1,013
Oxic	**Autoclaved (Sterile)**	900	111,814	7,160	Too Low	3180	NA		
			99,214		Too Low		Too Low		
	No naphthalene	2,820	10,460	6,260	10,234	1402	2,258		
			10,966		13,356		1,775		
	Experimental	1,932	1,555,558	2,800	1,062,640	776	88,624		
			1,703,553		1,016,104		140,810		
NO_3^{2-}	**Autoclaved (Sterile)**			1,466	83	492	28	171	NA
					35		Too Low		NA
	No Naphthalene			2,080	19,944	520	5,083	92.6	106
					21,207		5,533		55
	Experimental			10,800	123,344	5020	61,212	3,820	38,427
					135,520		63,556		40,887
SO_4^{2-}	**Autoclaved (Sterile)**			716	180	163	4,720	71.2	12,713
					101		4,922		10,258
	No Naphthalene			1,554	13,692	228	3,009	157	613
					12,165		2,791		604
	Experimental			1,952	15,564	308	27,907	254	404
					17,382		33,422		217
Fe^{3+}	**Autoclaved (Sterile)**			272	NA	Too Low	NA	14.2	NA
					Too Low		NA		NA
	No Naphthalene			1,804	20,324	111	2,161	300	678
					19,996		3,052		679
	Experimental			2,060	118,616	230	54,481	518	3,155
					132,771		51,583		2,485